D_4-flops of the E_7-model

Mboyo Esole[♠] and Sabrina Pasterski[†]

[♠] Department of Mathematics, Northeastern University
360 Huntington Avenue, Boston, MA 02115, USA
Email: j.esole@northeastern.edu

[†] Center for the Fundamental Laws of Nature, Harvard University
17 Oxford Street, Cambridge, MA 02138, USA
Email: spasterski@fas.harvard.edu

Abstract:

We study the geography of crepant resolutions of E_7-models. An E_7-model is a Weierstrass model corresponding to the output of Step 9 of Tate's algorithm characterizing the Kodaira fiber of type III* over the generic point of a smooth prime divisor. The dual graph of the Kodaira fiber of type III* is the affine Dynkin diagram of type $\widetilde{E}_7$. A Weierstrass model of type E_7 is conjectured to have eight distinct crepant resolutions whose flop diagram is a Dynkin diagram of type E_8. We construct explicitly four of these eight crepant resolutions forming a sub-diagram of type D_4. We explain how the flops between these four crepant resolutions can be understood using the flops between the crepant resolutions of two well-chosen suspended pinch points.

Keywords: Elliptic fibrations, Crepant morphisms, Resolution of singularities, Weierstrass models

Contents

1 Introduction

This paper aims to explore the geography of crepant resolutions of E_7-models given by singular Weierstrass models corresponding to Step 9 of Tate's algorithm [9, 40, 56]. In M-theory and F-theory compactifications, such geometries produce E_7 gauge theories (respectively in five- and six-dimensional spacetime with eight supersymmetric generators), with matter transforming in the adjoint and the fundamental representation of E_7 of dimension 56. We will denote that representation as **56** in the rest of the paper. Flops between distinct crepant resolutions are then interpreted as phase transitions between distinct Coulomb chambers of the $\mathcal{N} = 1$ five-dimensional gauge theory. The intersection polynomial is not invariant under flops and has to be computed in each of the crepant resolutions.

The last few years have seen a deep improvement of our understanding of the geography of crepant resolutions of Weierstrass models. Crepant resolutions of a singular Weierstrass model are relative minimal models (in the sense of Mori) over the Weierstrass model and are connected to each other by a finite sequence of flops. One significant incomplete problem at the boundary between birational geometry and string geometry is the explicit construction of all the crepant resolutions of a given Weierstrass model coming from Tate's algorithm [3]. The geography of these crepant resolutions is the study of the network of flops connecting them. It is natural to ask what is the geography of the minimal models corresponding to a given Weierstrass model: How many such minimal models are there? What is the graph of their flops?[1]

The systematic investigation of the geography of minimal models of Weierstrass models started with the study of the crepant resolutions of the SU(5)-model and has been completed for G-models with G a simple complex Lie group of low-rank such as $\mathrm{SU}(n)$ (for $n = 2, 3, 4, 5$) [33,34], G_2, Spin(7), Spin(8) [24], and F_4 [25]. Semi-simple cases and cases with non-trivial Mordell–Weil groups have also been investigated recently [28–30]. There are still some important omissions. With the exception of infinite series, E_5=Spin(10), E_6 and E_7 are the two crucial cases left for which the details of the crepant resolutions defining each chamber are still a mystery. The E_6-model corresponds to a Kodaira fiber $\mathrm{IV}^{*\mathrm{s}}$ covered by Step 8 of Tate's algorithm while the E_7-model corresponds to the Kodaira fiber III^* and step 9 of Tate's algorithm.

We would like to start a detailed exploration of the minimal models of the E_7-model. In this context, minimal models are crepant resolutions over the Weierstrass model. We would like to explicitly construct each minimal model over the Weierstrass model as a projective variety defined by a crepant resolution of the Weierstrass model of an E_7-model and study the geography of these different crepant resolutions. An E_7 Weierstrass model is conjectured to have eight distinct crepant resolutions whose flop diagram is a Dynkin diagram of type E_8. However, to this day, these crepant resolutions have not been identified. We will construct four of the eight conjectured minimal models of an E_7-model and show that their flops define a Dynkin diagram of type D_4. In our construction, the birational geometry of the suspended pinch point will be used to model the flops of the minimal

[1] We attach a graph to the collection of minimal models of a Weierstrass model such that the nodes of the graph are in bijection with the minimal models and two nodes are connected by an edge when the two corresponding minimal models are connected by a flop. Such a graph is called the *graph of flops of the minimal models*. If the elliptic fibration is a Calabi-Yau threefold, the graph of flops corresponds to the incidence graph of the distinct chambers of the Coulomb branch of the five-dimensional gauge theory obtained by a compactification of M-theory on the elliptic fibration.

models we discuss.

1.1 Defining the E_7-model

An E_7-model is an elliptic fibration $Y \longrightarrow B$ over a smooth base B with a choice of a smooth prime divisor S in the base B such that the fiber over the generic point of S is of Kodaira type III* and all singular fibers over generic points of the discriminant locus away from S are irreducible (of Kodaira type II or I_1). The name "E_7-model" stems from the fact that the dual graph of a Kodaira fiber [42] of type III* is the affine Dynkin diagram of type $\widetilde{E}_7$. E_7-models are typically given by singular Weierstrass models using Step 9 of Tate's algorithm, which can be traced to Proposition 4 of Néron's thesis [48].

Let B be a smooth variety of dimension two or higher over the complex numbers. Given a line bundle $\mathscr{L}$, we define the projective bundle of lines $\pi : X_0 = \mathbb{P}_B[\mathscr{O}_B \oplus \mathscr{L}^{\otimes 2} \oplus \mathscr{L}^{\otimes 3}] \to B$. The projective bundle X_0 is the ambient space for a Weierstrass model [20]. Let $\mathscr{O}_{X_0}(1)$ be the dual of the tautological line bundle of X_0, a Weierstrass model is by definition the zero scheme of a section of the line bundle $\mathscr{O}_{X_0}(3) \otimes \pi^*\mathscr{L}^{\otimes 6}$. Throughout this paper, we work over the complex numbers $\mathbb{C}$. Given sections f_i of lines bundles $\mathscr{L}_i$, we denote by $V(f_1, \ldots, f_r)$ their vanishing scheme defined as the zero scheme $f_1 = f_2 = \cdots = f_r = 0$. If we denote the relative projective coordinates of X_0 as $[z : x : y]$, a Weierstrass model is the following vanishing locus

$$V(y^2z - x^3 - fxz^2 - gz^3),$$

where f is a section of $\mathscr{L}^{\otimes 4}$ and g is a section of $\mathscr{L}^{\otimes 6}$. The discriminant and the j-invariant are given by the following expressions

$$\Delta = 4f^3 + 27g^2, \quad j = 1728\frac{4f^3}{\Delta}.$$

The divisor Δ is a section of the line bundle $\mathscr{L}^{\otimes 12}$. The locus of points of B over which the fiber is singular is $V(\Delta)$. The fibers of a smooth Weierstrass model are all irreducible of type I_0 (smooth elliptic curve), I_1 (nodal elliptic curve), and II (cuspidal elliptic curve). Reducible fibers appear only after resolving the singularities of a singular Weierstrass model up to codimension-two.

The general Weierstrass equation is [16]

$$y^2z + a_1xyz + a_3yz^2 - x^3 - a_2x^2z - a_4xz^2 - a_6z^3 = 0. \tag{1.1}$$

Let $S = V(s)$ be a smooth and irreducible Cartier divisor in a smooth variety B. We denote the generic point of S and its residue field by η and κ, respectively. We define a valuation v_S such that $v_S(f) = n$ when a rational function f has a zero of multiplicity n if $n \geq 0$ or a pole of multiplicity $-n$ if $n < 0$.

An E_7-model is characterized by Step 9 of Tate's algorithm and corresponds to type (c7) in Néron's classification [48]. Following Proposition 4 of [48], an E_7-model is characterized by the

following restrictions on the valuations of the coefficients of the Weierstrass equation:

$$v_S(a_1) \geq 1, \quad v_S(a_2) \geq 2, \quad v_S(a_3) \geq 3, \quad v_S(a_4) = 3, \quad v_S(a_6) \geq 5. \tag{1.2}$$

After completing the square in y and the cube in x, an elliptic fibration with generic fiber of Kodaira type III* over $S = V(s)$ can always be written as the following Weierstrass model

$$y^2 z = x^3 + a_{4,3} s^3 x z^2 + a_{6,5+\beta} s^{5+\beta} z^3, \quad \beta \in \mathbb{Z}_{\geq 0}, \tag{1.3}$$

where $a_{i,j}$ is a section of $\mathscr{L}^{\otimes i} \otimes \mathscr{S}^{-\otimes j}$ where $\mathscr{S} = \mathscr{O}_B(S)$. Such an elliptic fibration is called an E_7-model. In this paper, we focus on the case $\beta = 0$ and, to ease the notation, we will write the Weierstrass model as follows

$$y^2 z = x^3 + a s^3 x z^2 + b s^5 z^3, \tag{1.4}$$

where $S = V(s)$ is a smooth Cartier divisor defined by the zero locus of a section of the line bundle $\mathscr{S}$, a is a section of $\mathscr{L}^{\otimes 4} \otimes \mathscr{S}^{-\otimes 3}$, and b is a section of $\mathscr{L}^{\otimes 6} \otimes \mathscr{S}^{-\otimes 5}$. We assume that a and b have zero valuation along S and $V(a)$ and $V(b)$ are smooth divisors in B intersecting transversally.

The discriminant locus of this Weierstrass model is the vanishing scheme of Δ with

$$\Delta = s^9 (4a^3 + 27 b^2 s). \tag{1.5}$$

The reduced discriminant locus consists of two prime divisors, namely

$$S = V(s) \quad \text{and} \quad \Delta' = V(4a^3 + 27 b^2 s). \tag{1.6}$$

The divisor Δ' has cuspidal singularities at $V(a, b)$ that worsen to triple point singularities over $V(a, b, s)$. The divisors S and Δ' do not intersect transversally as their intersection scheme consists of triple points (s, a^3). Since the generic point of Δ' is regular, we can still apply Tate's algorithm along Δ'. The fiber over the generic point of S has Kodaira type III* and the generic fiber over Δ' is of Kodaira type I_1. The collision of singularities III*+I_1 is not in the list of Miranda as the two fibers have distinct j-invariant. We do expect a degeneration of the fiber III* over the the codimension-two locus $V(s, a)$ of the base B and further at the codimension-three loci $V(s, a, b)$.

1.2 E_7 facts and conjectures

In this section, we recall some facts and conjectures about the E_7-model that are relevant to appreciate the questions addressed in this paper.

1. **Topological invariants.** The Hodge numbers and the Euler characteristic of a crepant resolution are invariant under flops and can therefore be computed in any crepant resolution. The Euler characteristic over a base of arbitrary dimension of an E_7-model has been computed in [26]. The Hodge numbers and the Euler characteristic of an E_7-model in the special case of an elliptically fibered Calabi-Yau threefold that is obtained by a crepant resolution of a Weierstrass model are independent of the choice of crepant resolution [7] and are given in [26].

The key point is that the Euler characteristic is

$$\chi = -60K^2 - 98K \cdot S - 42S^2 = -60K^2 + 196(1-g) + 56S^2.$$

The characteristic numbers of an E_7-model are computed in [27]. See also [21, 31].

2. **Singular fibers of fibral divisors and the minuscule representation 56.** The fiber of type III* degenerates over the collision of S and Δ'. The irreducible rational curves forming the singular fiber over $S \cap \Delta'$ have geometric weights in the representation **56** of E_7, which is a minuscule fundamental representation. Thus, the matter representation associated with an E_7-model is the direct sum of the adjoint (**133**) and the fundamental representation (**56**) of E_7.

3. **Non-Higgsable cluster.** The representation **56** does not occur when S and Δ' do not intersect. This is famously illustrated by the non-Higgsable cluster corresponding to the local Calabi-Yau threefold defined over the quasi-projective surface given by the total space of the line bundle $\mathscr{O}_{\mathbb{P}^1}(-8)$. See [6, 17, 47].

4. **Loss of flatness.** When the base of the fibration is at least of dimension three, a crepant resolution of the E_7-model does not give a flat fibration over the base as there are codimension-three points over which the fiber contains a full quadric surface as discussed in the partial toric resolutions of [14]. We will see that this happens exactly over the intersection of S with the singular locus of Δ', namely over the codimension-three locus $V(s, a, b)$ in the base B.

5. **The geography of crepant resolutions.** The authors of [38] conjectured that there are eight crepant resolutions of the Weierstrass model of an E_7-model and the graph of their flops is a Dynkin diagram of type E_8. This is based on studying the hyperplane arrangement defined by the weights of the representation **56** inside the dual fundamental Weyl chamber of E_7. The crepant resolutions were not constructed explicitly. See also [18].

6. **The fiber structure.** The authors of [38] also conjectured that the crepant resolution corresponding to the α_i of E_8 is such that the generic fiber over S degenerates over $V(a)$ to a non-Kodaira fiber whose dual graph is the same as the affine Dynkin diagram of type $\widetilde{\mathrm{E}}_8$ with the node α_i contracted to a point. This has not been verified geometrically in more than one chamber.

1.3 Summary of results

The key results of this paper are the following:

1. We give four distinct crepant resolutions of the Weierstrass model of the E_7-model. We show that the graph of the flops between these four crepant resolutions is a D_4-Dynkin subdiagram of the expected E_8 flop-diagram as illustrated in Figure 1.1. More specifically the resolutions correspond to the nodes α_4, α_5, α_6, and α_8 of the Dynkin diagram of type E_8 of Figure 1.1. For that reason, we call these resolutions Y_4, Y_5, Y_6, and Y_8, respectively. We show that the D_4-Dynkin diagram of flops can be understood by the flops of two suspended pinch points as illustrated on Figure 4.9.

2. We show that in the resolution Y_i $(i = 4, 5, 6, 8)$, the generic fiber over $V(s, a)$ corresponds to the Dynkin diagram of type $\widetilde{\mathrm{E}}_8$ with the node α_i contracted to a point.

3. For each resolution, we identify the new curves that appear over $V(s, a)$. They are extreme rays of the resolution and their geometric weights are always in the minuscule representation **56**. In particular, we find the five extreme rays corresponding to the weights ϖ_{23}, ϖ_{26}, ϖ_{29}, ϖ_{30}, ϖ_{32} as illustrated on Figure 1.1.

4. We also show that in each of the four crepant resolutions studied in this paper, the divisor D_6 corresponding to the root α_6 has a fiber that jumps in dimension over the codimension-three locus $V(s, a, b)$. All other fibers are always one dimensional over any point of the base.

5. We compute the triple intersection numbers of the fibral divisors and in this way give a geometric derivation of the Chern-Simons levels and of the superpotential of an E_7-model in the four chambers studied in this paper.

6. We compute the number of hypermultiplets in an M-theory compactification on a Calabi-Yau threefold that is an E_7-model by comparing the triple intersection numbers with the one-loop corrected superpotential of a five-dimensional supergravity theory with Lie group E_7 and matter transforming in the adjoint and the fundamental representation **56** [39]. As expected, the number of adjoints is the genus of the curve supporting the fiber III* and the number of fundamentals is given by the number of intersection points between the two irreducible components of the reduced discriminant locus:

$$n_{\mathbf{133}} = g, \quad n_{\mathbf{56}} = \frac{1}{2} S \cdot [a] = \frac{1}{2}\Big(8(1-g) + S^2\Big).$$

   But this intersection is not transverse as S and Δ' intersect along the scheme (s, a^3) which consists of triple points supported on $V(s, a)$. The factor of $1/2$ indicates that each intersection point contributes one half-hypermultiplet, which is possible because the representation **56** is pseudo-real. When S is a rational curve, $n_{\mathbf{133}} = 0$. If S is a rational curve of self-intersection $S^2 = -8$, we get $\mathrm{n}_{\mathbf{56}} = 0$ while when it is a rational curve of self-intersection $S^2 = -7$ we get $\mathrm{n}_{\mathbf{56}} = 1/2$, which corresponds to a unique half-hypermultiplet.

For convenience, we collect our results in the following pages.

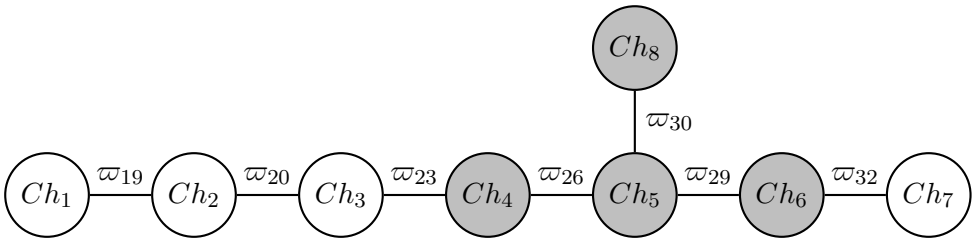

Figure 1.1: Adjacency graph of the chambers of the hyperplane arrangement I(E_7, **56**). Each chamber is simplicial. A weight ϖ between two nodes indicates that the corresponding chambers are separated by the hyperplane $\varpi^\perp$. For example, one goes from Ch_1 to Ch_2 by crossing the hyperplane $\varpi_{19}^\perp$. The colored chambers forming a subgraph of type D_4 are those corresponding to the nef-cone of the crepant resolutions constructed in this paper.

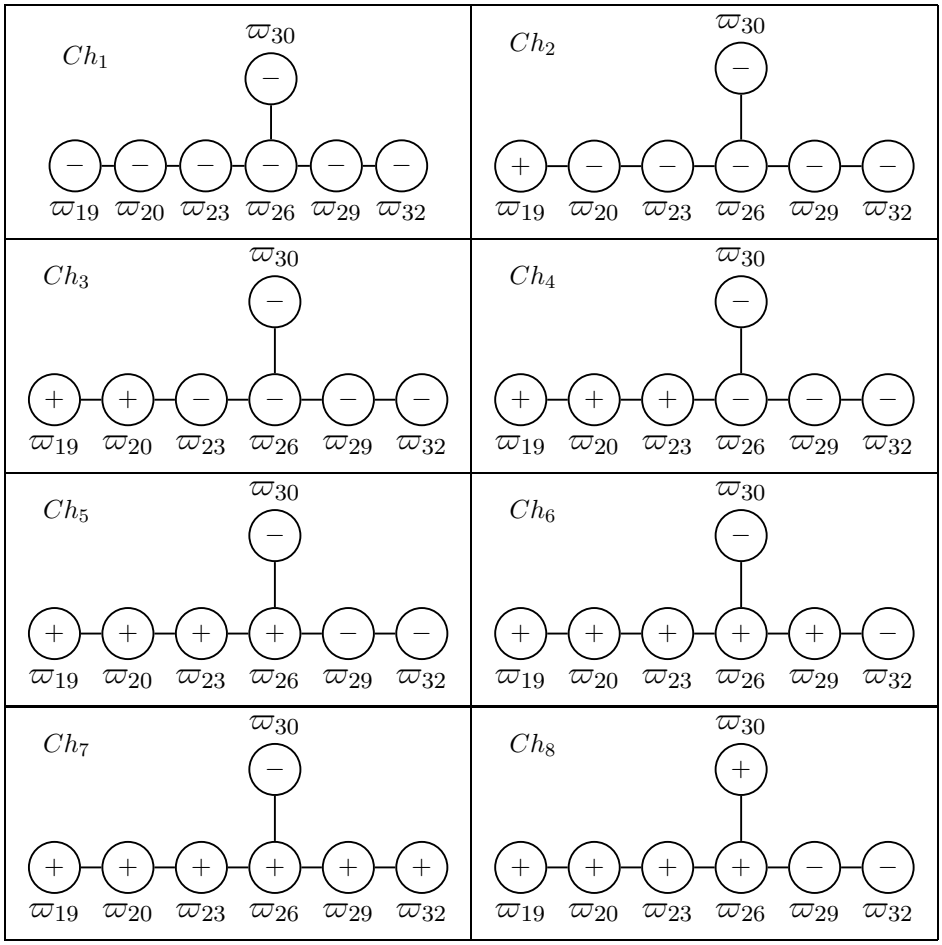

Table 1: The eight chambers of I(E_7, **56**). Each chamber is uniquely defined by the signs taken by the seven linear functions $\langle \varpi_i, \phi \rangle$ for $i = \{19, 20, 23, 26, 29, 32, 30\}$. Together, they define a sign vector for the hyperplane arrangement. These weights satisfy a partial order whose Hasse diagram is a Dynkin diagram of type E_7 as illustrated in Figure 3.4.

Chamber 4	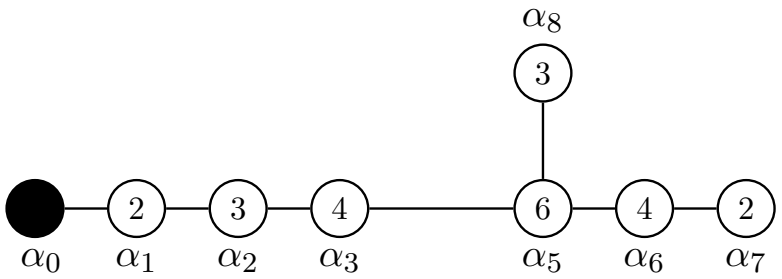
Chamber 5	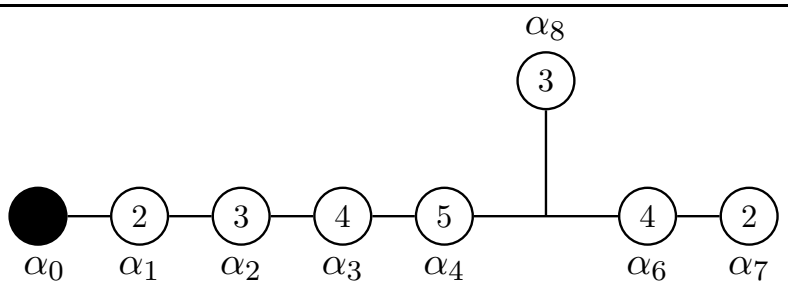
Chamber 6	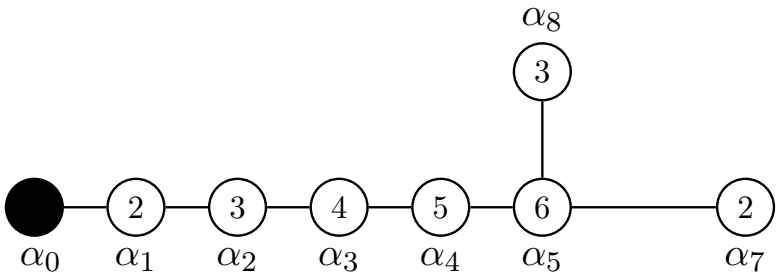
Chamber 8	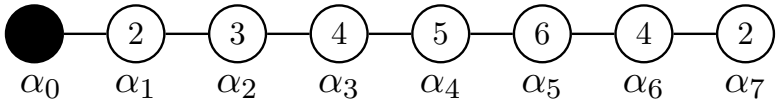

Table 2: Degeneration of the E_7-fiber over $V(s,a)$. These fibers should be compared with the affine Dynkin diagram of type $\widetilde{E}_8$ in Figure 3.2. The degenerated fiber is a Kodaira fiber of type II* with a node contracted to a point. In each chamber, the node that is contracted is different. These fibers are computed directly from explicit crepant resolutions of singularities.

$$
\begin{aligned}
6\mathcal{F}_1(\phi) = {} & 2(1-n_A)\left(4\phi_1^3+3\phi_2\phi_1^2-6\phi_2^2\phi_1+4\phi_2^3+4\phi_3^3+4\phi_4^3+4\phi_5^3+4\phi_6^3+4\phi_7^3\right.\\
& \left.-3\phi_2\phi_3^2+3\phi_4\phi_5^2+6\phi_5\phi_6^2-3\phi_3^2\phi_4-6\phi_4^2\phi_5-9\phi_5^2\phi_6-3\phi_3^2\phi_7\right)\\
& -2n_F\phi_6\left(6\phi_1^2-6\phi_2\phi_1+6\phi_2^2+6\phi_3^2+6\phi_4^2\right.\\
& \left.+6\phi_5^2+5\phi_6^2+6\phi_7^2-6\phi_2\phi_3-6\phi_3\phi_4-6\phi_4\phi_5-6\phi_5\phi_6-6\phi_3\phi_7\right)
\end{aligned}
$$

$$
\begin{aligned}
6\mathcal{F}_2(\phi) = {} & 2(1-n_A)\left(4\phi_1^3+3\phi_2\phi_1^2-6\phi_2^2\phi_1+4\phi_2^3+4\phi_3^3+4\phi_4^3+4\phi_5^3+4\phi_6^3\right.\\
& \left.+4\phi_7^3-3\phi_2\phi_3^2+3\phi_4\phi_5^2+6\phi_5\phi_6^2-3\phi_3^2\phi_4-6\phi_4^2\phi_5-9\phi_5^2\phi_6-3\phi_3^2\phi_7\right)\\
& -2n_F\left(\phi_1^3+3\phi_6\phi_1^2+3\left(\phi_6-2\phi_2\right)\phi_6\phi_1+2\phi_6\left(3\phi_2^2-3\phi_3\phi_2+\right.\right.\\
& \left.\left.3\phi_3^2+2\phi_6^2+3\phi_7^2+3\left(\phi_4^2-\phi_5\phi_4+\phi_5^2\right)-3\phi_5\phi_6-3\phi_3(\phi_4+\phi_7)\right)\right)
\end{aligned}
$$

$$
\begin{aligned}
6\mathcal{F}_3(\phi) = {} & 2\left(1-n_A\right)\left(4\phi_1^3+3\phi_2\phi_1^2-6\phi_2^2\phi_1+4\phi_2^3+4\phi_3^3+4\phi_4^3+4\phi_5^3+4\phi_6^3\right.\\
& \left.+4\phi_7^3-3\phi_2\phi_3^2+3\phi_4\phi_5^2+6\phi_5\phi_6^2-3\phi_3^2\phi_4-6\phi_4^2\phi_5-9\phi_5^2\phi_6-3\phi_3^2\phi_7\right)\\
& -2n_F\left(\phi_2^3-3\phi_1\phi_2^2+3\phi_6\phi_2^2+3\phi_1^2\phi_2+3(\phi_6-2\phi_3)\phi_6\phi_2\right.\\
& \left.+3\phi_6(2\phi_3^2-2(\phi_4+\phi_7)\phi_3+\phi_6^2+2\phi_7^2+2(\phi_4^2-\phi_5\phi_4+\phi_5^2)-2\phi_5\phi_6)\right)
\end{aligned}
$$

$$
\begin{aligned}
6\mathcal{F}_4(\phi) = {} & 2(1-n_A)(4\phi_1^3+3\phi_2\phi_1^2-6\phi_2^2\phi_1+4\phi_2^3+4\phi_3^3+4\phi_4^3+4\phi_5^3\\
& +4\phi_6^3+4\phi_7^3-3\phi_2\phi_3^2+3\phi_4\phi_5^2+6\phi_5\phi_6^2-3\phi_3^2\phi_4-6\phi_4^2\phi_5-9\phi_5^2\phi_6-3\phi_3^2\phi_7)\\
& -2n_F(\phi_3^3-3\phi_2\phi_3^2+3\phi_6\phi_3^2+3\phi_2^2\phi_3+3\phi_6^2\phi_3-6\phi_4\phi_6\phi_3-6\phi_6\phi_7\phi_3+2\phi_6^3\\
& -3\phi_1\phi_2^2-6\phi_5\phi_6^2+6\phi_6\phi_7^2+3\phi_1^2\phi_2+6\phi_4^2\phi_6+6\phi_5^2\phi_6-6\phi_4\phi_5\phi_6)
\end{aligned}
$$

$$
\begin{aligned}
6\mathcal{F}_5(\phi) = {} & 2(1-n_A)(4\phi_1^3+3\phi_2\phi_1^2-6\phi_2^2\phi_1+4\phi_2^3+4\phi_3^3+4\phi_4^3+4\phi_5^3+4\phi_6^3\\
& +4\phi_7^3-3\phi_2\phi_3^2+3\phi_4\phi_5^2+6\phi_5\phi_6^2-3\phi_3^2\phi_4-6\phi_4^2\phi_5-9\phi_5^2\phi_6-3\phi_3^2\phi_7)\\
& -2n_F(\phi_4^3-3\phi_3\phi_4^2+3\phi_6\phi_4^2+3\phi_3^2\phi_4+3\phi_6^2\phi_4-6\phi_5\phi_6\phi_4+\phi_6^3+\phi_7^3-3\phi_1\phi_2^2-3\phi_2\phi_3^2-6\phi_5\phi_6^2\\
& +3(-\phi_3+\phi_4+\phi_6)\phi_7^2+3\phi_1^2\phi_2+3\phi_2^2\phi_3+6\phi_5^2\phi_6+3((\phi_3-\phi_4)^2+\phi_6^2-2\phi_4\phi_6)\phi_7)
\end{aligned}
$$

$$
\begin{aligned}
6\mathcal{F}_6(\phi) = {} & 2(1-n_A)(4\phi_1^3+3\phi_2\phi_1^2-6\phi_2^2\phi_1+4\phi_2^3+4\phi_3^3+4\phi_4^3+4\phi_5^3+4\phi_6^3\\
& +4\phi_7^3-3\phi_2\phi_3^2+3\phi_4\phi_5^2+6\phi_5\phi_6^2-3\phi_3^2\phi_4-6\phi_4^2\phi_5-9\phi_5^2\phi_6-3\phi_3^2\phi_7)\\
& -2n_F(\phi_5^3-3\phi_4\phi_5^2+3\phi_6\phi_5^2+3\phi_4^2\phi_5-3\phi_6^2\phi_5+2\phi_7^3-3\phi_1\phi_2^2\\
& -3\phi_2\phi_3^2-3\phi_3\phi_4^2+3(\phi_5-\phi_3)\phi_7^2+3\phi_1^2\phi_2+3\phi_2^2\phi_3\\
& +3\phi_3^2\phi_4+3(\phi_3^2-2\phi_4\phi_3+2\phi_4^2+\phi_5^2+2\phi_6^2-2\phi_4\phi_5-2\phi_5\phi_6)\phi_7)
\end{aligned}
$$

$$
\begin{aligned}
6\mathcal{F}_7(\phi) = {} & 2(1-n_A)(4\phi_1^3+3\phi_2\phi_1^2-6\phi_2^2\phi_1+4\phi_2^3+4\phi_3^3+4\phi_4^3+4\phi_5^3+4\phi_6^3\\
& +4\phi_7^3-3\phi_2\phi_3^2+3\phi_4\phi_5^2+6\phi_5\phi_6^2-3\phi_3^2\phi_4-6\phi_4^2\phi_5-9\phi_5^2\phi_6-3\phi_3^2\phi_7)\\
& -6n_F(\phi_7^3-\phi_3\phi_7^2+(\phi_3^2-2\phi_4\phi_3+2(\phi_4^2-\phi_5\phi_4+\phi_5^2+\phi_6^2-\phi_5\phi_6))\phi_7\\
& -\phi_1\phi_2^2-\phi_2\phi_3^2-\phi_3\phi_4^2-\phi_4\phi_5^2-\phi_5\phi_6^2+\phi_1^2\phi_2+\phi_2^2\phi_3+\phi_3^2\phi_4+\phi_4^2\phi_5+\phi_5^2\phi_6)
\end{aligned}
$$

$$
\begin{aligned}
6\mathcal{F}_8(\phi) = {} & 2(1-n_A)(4\phi_1^3+3\phi_2\phi_1^2-6\phi_2^2\phi_1+4\phi_2^3+4\phi_3^3+4\phi_4^3+4\phi_5^3+4\phi_6^3+4\phi_7^3\\
& -3\phi_2\phi_3^2+3\phi_4\phi_5^2+6\phi_5\phi_6^2-3\phi_3^2\phi_4-6\phi_4^2\phi_5-9\phi_5^2\phi_6-3\phi_3^2\phi_7)\\
& -2n_F(2\phi_4^3-3\phi_3\phi_4^2+3\phi_3^2\phi_4+6\phi_6^2\phi_4-6\phi_5\phi_6\phi_4-3\phi_1\phi_2^2-3\phi_2\phi_3^2\\
& -6\phi_5\phi_6^2-3(\phi_3-2\phi_4)\phi_7^2+3\phi_1^2\phi_2+3\phi_2^2\phi_3+6\phi_5^2\phi_6+3\phi_3(\phi_3-2\phi_4)\phi_7)
\end{aligned}
$$

Table 3: Prepotential in the eight chambers of the Coulomb branch of E_7 with n_A hypermultiplet charged in the adjoint representation (**133**) and n_F hypermultiplets charged in the fundamental representation (**56**).

2 Preliminaries

2.1 G-models and Coulomb phases

Let $\varphi : X \longrightarrow B$ be an elliptic fibration defined over the complex numbers, so that φ is a proper morphism between complex quasi-projective varieties. We will assume that the base B of the fibration is a smooth complex variety and denote the discriminant locus by Δ. Under mild assumptions, Δ is a Cartier divisor.

Inspired by the physics of F-theory, we attach to the elliptic fibration $\varphi : Y \longrightarrow B$ a unique reductive complex Lie group G and a representation $\mathbf{R}$ of its Lie algebra $\mathfrak{g} = \mathrm{Lie}(G)$. The Lie algebra $\mathfrak{g}$ is uniquely defined by the dual graphs of the singular fibers of φ over the generic points of its discriminant locus Δ, and φ is referred to as a *G-model*.[2]

The irreducible components of the singular fibers over codimension-two points of the base determine a finite set of weights belonging to the representation $\mathbf{R}$. Determining $\mathbf{R}$ from these weights is particularly straightforward when $\mathbf{R}$ is a (quasi)-minuscule representation, as in that case all the (nonzero) weights of $\mathbf{R}$ are then by definition in the same Weyl orbit. The group G is such that its first homotopy group is isomorphic to the Mordell–Weil group of φ, and $\mathbf{R}$ is a representation of G. Several aspects of the geometry of the elliptic fibration φ are controlled by the triple $(\mathfrak{g}, G, \mathbf{R})$.

M-theory compactified on a Calabi–Yau threefold given by a G-model results in an $\mathcal{N} = 1$ five-dimensional gauged supergravity theory with gauge group G. In the language of five-dimensional supersymmetric gauge theories with eight supercharges, each distinct crepant resolution of the Weierstrass model corresponds to a different chamber of the Coulomb branch of the theory. String dualities suggest that the graph of flops between distinct minimal models is isomorphic to the adjacency graph of the chambers of the hyperplane arrangement $\mathrm{I}(\mathfrak{g}, \mathbf{R})$ whose hyperplanes are the kernels of the weights of the representation $\mathbf{R}$ restricted to the dual fundamental Weyl chamber of $\mathfrak{g}$. This picture requires that the elliptic fibration is a Calabi-Yau threefold, but we expect that the hyperplane arrangement is valid in a larger setup than the Calabi-Yau threefold case and even relevant to study varieties more general than elliptic fibrations. For example, it can be extended to the case of $\mathbb{Q}$-factorial terminal singularities that are partial resolutions of threefolds with cDV singularities.

2.2 Geography of minimal models: decomposition of the relative movable cone into relative nef-cones.

The description of the Coulomb branch of a five-dimensional gauge theory with gauge algebra $\mathfrak{g}$ and a representation $\mathbf{R}$ in terms of a hyperplane arrangement $\mathrm{I}(\mathfrak{g}, \mathbf{R})$ is strikingly similar to the point of view of birational geometers who rely on several cones to describe the birational geometry of projective varieties in the same birational class. In particular, we refer to Section 12.2 of Matsuki [45] and to Kawamata's seminal paper [41] for a description of the relative movable cone and

[2] If Δ_i are the irreducible components of the reduced discriminant and p_i is the generic point of Δ_i, the Langlands dual of the dual graph of the fiber over p_i has an affine Dynkin type $\widetilde{\mathfrak{g}}_i$ and the Lie algebra $\mathfrak{g}$ is the direct sum $\mathfrak{g} = \bigoplus_i \mathfrak{g}_i$. By definition, the Kodaira type associated to a component Δ_i is the type of the geometric fiber over p_i. The dual graph of a Kodaira fiber is always an affine Dynkin diagram of type ADE. We assume that at least one component Δ_i of the reduced discriminant has a reducible fiber over its generic point, that is, a Kodaira fiber of type different from type II and type I_1.

its decomposition theorem into relative nef-cones.

Let $\varphi : Y \longrightarrow B$ be an elliptic fibration. Let $f : Y \to W$ be the birational map to its Weierstrass model. Then f contracts all fibral divisors not touching the zero section of the fibration. In the case of an elliptic surface, that is enough to see that the Weierstrass model is the canonical model of Y. When an elliptic fibration has a trivial Mordell-Weil group, the fibral divisors D_m and the zero section generate the relative Néron-Severi cone $\mathrm{N}^1(X/B)$.

Given a crepant resolution $f : X \longrightarrow W$ of a Weierstrass model, the relative Picard number $\rho(X/W)$ gives the rank of the gauge group and $\mathrm{N}^1(X/W)$ is generated by the fibral divisors D_m not touching the zero section. Each relative one-cycle $\varpi(C)$ defines a map $\mathrm{N}^1(X/W) \to \mathbb{Z}^{\rho(X/W)}$ via the intersection. The geometric weights of a relative 1-cycle C is a vector $\varpi(C) \in \mathbb{Z}^{\rho(X/W)}$ given by the negative of the intersection numbers with the fibral divisors not touching the section of the elliptic fibration [4, 24]:

$$\varpi_m(C) = -\int_X D_i \cdot C,$$

where D_i are the fibral divisors not touching the section of the elliptic fibration. Each relative one-cycle defines a hyperplane in $\mathrm{N}^1(X/W)$:

$$\varpi^{\perp}(C) = \{D \in \mathrm{N}^1(X/W) | \int_X (D \cdot C) = 0\}.$$

Each divisor D_i is a fibration over S and we denote its generic fiber by C_i. The curves C_i generate an open convex cone in $\mathrm{N}^1(X/W)$. We denote the open dual cone in $\mathrm{N}^1(X/W)$ by $\mathfrak{D}$:

$$\mathfrak{D} = \{D \in \mathrm{N}^1(X/W) | \quad \forall i \int_X (D \cdot C_i) \geq 0\} = \bigcap_{i=1}^{\rho(X/W)} (C_i)_{\geq 0}.$$

This cone corresponds to the dual Weyl chamber of $\mathfrak{g}$. Geometrically, we expect $\mathfrak{D}$ to be the cone of relative movable divisors $\overline{\mathrm{Mov}}(X/W)$.

A pseudo-isomorphism is a birational map that is an isomorphism in codimension-one. A small $\mathbb{Q}$-factorial modification (SQM) is a pseudo-isomorphism between $\mathbb{Q}$-factorial projective varieties. Given a SQM between two varieties X_1 and X_2, we get naturally an associated identifcation of the of the Néron-Severi groups $\mathrm{N}^1(X_1)$ and $\mathrm{N}^1(X_2)$ via pullback and pushforward.

Any nef-divisor is movable and the partition theorem implies that any movable divisor becomes nef after a finite number of flops. For any two $\mathbb{Q}$-factorial varieties Y_1 and Y_2 related by a birational map that is an isomorphism in codimension-one, the cones $\mathrm{N}^1(Y_1/W)$ and $\mathrm{N}^1(Y_2/W)$ can be canonically identified by pushforward and pullback. We also identify in this way some other important subcones of $\mathrm{N}^1(Y/W)$ and $\mathrm{N}^1(Y/W)$ such as the relative movable cones $\mathrm{Mov}(Y/W)$, the ample cones $\mathrm{Amp}(Y/W)$, and the big cones $\mathrm{Big}(Y/W)$

$$\overline{\mathrm{Amp}}(Y/S) \subset \overline{\mathrm{Mov}}(Y/S) \subset \overline{\mathrm{Big}}(Y/S) \subset \mathrm{N}^1(Y/S).$$

The closure of the ample cone is the nef-cone. In ideal cases, we expect that the relative movable cone decomposes as a union of relative nef-cones of all the minimal models in the same birational

orbit:

$$\overline{\mathrm{Mov}}(Y/S) = \bigsqcup_i \overline{\mathrm{Amp}}(Y_i/S),$$

where the union is over all minimal models in the same birational class of Y and the interiors of the cones $\overline{\mathrm{Amp}}(Y_i/S)$ are disjoint.

Since the pullback of an ample divisor is movable, the identification of $\mathrm{N}^1(X_1)$ and $\mathrm{N}^1(X_2)$ also embeds the ample cone of X_2 onto a subcone of the movable cone of X_1. The partition theorem states that if we fix a given minimal model X, the nef-cones of the other minimal models X_i embedded into subcones of the movable cone of X will provide a partition of the movable cone of X.

The hyperplane arrangement $\mathrm{I}(\mathfrak{g}, \mathbf{R})$ describes the decomposition of the closed relative movable cone into relative nef-cones corresponding to each individual distinct crepant resolution.

Elliptic fibration	Hyperplane arrangement	Cones
Weierstrass model	Closed dual Weyl chamber of $\mathfrak{g}$	$\overline{\mathrm{Mov}}(Y/S)$
Crepant resolution	Chambers of $\mathrm{I}(\mathfrak{g}, \mathbf{R})$	$\overline{\mathrm{Amp}}(Y_i/S)$

3 The hyperplane arrangement $\mathrm{I}(\mathrm{E}_7, \mathbf{56})$

In this section, we review the construction of the root systems E_7, E_8, and the fundamental representation **56** of E_7. We then study the chamber structure of the hyperplane arrangement $\mathrm{I}(\mathrm{E}_7, \mathbf{56})$.

3.1 E_7 root system and Dynkin diagram

The Lie algebra of type E_7 has dimension 133 and rank 7: it has 126 distinct roots and its Cartan subalgebra has dimension 7. Its Weyl group has order $2^{10} \cdot 3^4 \cdot 5 \cdot 7$ [11, Plate VI]. The Coxeter number of the Lie algebra of type E_7 is 18. The determinant of the Cartan matrix of the Lie algebra of type E_7 is 2. Hence, the fundamental group of the root system of type E_7 and the quotient of the weight lattice modulo the root lattice are both isomorphic to $\mathbb{Z}/2\mathbb{Z}$.

A choice of positive simple roots is

$$\begin{array}{lll}
\alpha_1 = \frac{1}{2}(1,-1,-1,-1,-1,-1,-1,1), & & \\
\alpha_2 = (-1,1,0,0,0,0,0,0), & \alpha_3 = (0,-1,1,0,0,0,0,0), & \alpha_4 = (0,0,-1,1,0,0,0,0), \\
\alpha_5 = (0,0,0,-1,1,0,0,0), & \alpha_6 = (0,0,0,0,-1,1,0,0), & \alpha_7 = (1,1,\ 0,\ 0,0,0,0,0).
\end{array}$$

The Cartan matrix of E_7 is then

$$\begin{array}{c} \\ \alpha_1 \\ \alpha_2 \\ \alpha_3 \\ \alpha_4 \\ \alpha_5 \\ \alpha_6 \\ \alpha_7 \end{array} \begin{pmatrix} 2 & -1 & 0 & 0 & 0 & 0 & 0 \\ -1 & 2 & -1 & 0 & 0 & 0 & 0 \\ 0 & -1 & 2 & -1 & 0 & 0 & -1 \\ 0 & 0 & -1 & 2 & -1 & 0 & 0 \\ 0 & 0 & 0 & -1 & 2 & -1 & 0 \\ 0 & 0 & 0 & 0 & -1 & 2 & 0 \\ 0 & 0 & -1 & 0 & 0 & 0 & 2 \end{pmatrix} \tag{3.1}$$

The ith row of this Cartan matrix gives the coordinates of the simple root α_i in the basis of simple fundamental weights. In Bourbaki's tables, our simple roots $(\alpha_1, \alpha_2, \alpha_3, \alpha_4, \alpha_5, \alpha_6, \alpha_7)$ are denoted $(\alpha_1, \alpha_3, \alpha_4, \alpha_5, \alpha_6, \alpha_7, \alpha_2)$, respectively.

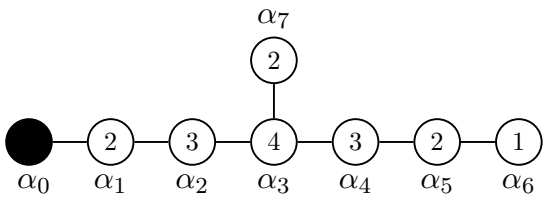

Figure 3.1: Affine Dynkin diagram of type $\widetilde{\mathrm{E}}_7$. Removing the black node gives the Dynkin diagram of type E_7. The numbers inside the nodes are the multiplicities of the Kodaira fiber of type III* and the Dynkin labels of the highest root. Thus, the Coxeter number of E_7 is 18. The root α_1 is the highest weight of the adjoint representation while α_6 is the highest weight of the fundamental represenation **56**.

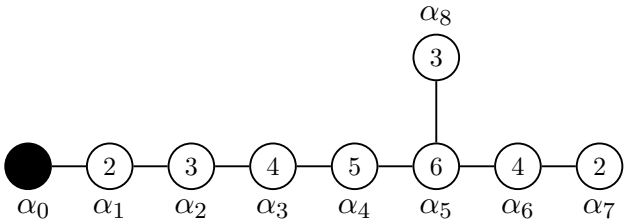

Figure 3.2: Affine Dynkin diagram of type $\widetilde{\mathrm{E}}_8$. Removing the black node gives the Dynkin diagram of type E_8. The number in the nodes are the multiplicities of the Kodaira fiber of type II*.

3.2 Root system of types E_7 and E_8, and representation 56 of E_7.

We now give a quick description of the root system of type E_7 and the weight system **56** of E_7 in terms of the root system of type E_8. We follow Borcherds's lecture notes on Lie groups [10].

The smallest non-trivial representation of E_7 is of dimension 56 and often called the fundamental representation. The representation **56** of E_7 is minuscule, self-dual, and pseudo-real. Its highest weight is the simple root α_6 (see Figure 3.1). The roots of E_8 form the unique eight dimensional even unimodular lattice. The roots of E_8 are the vertices of the Gosset polytope ($\mathbf{4_{21}}$ in Coxeter's notation). The roots of $\mathfrak{e}_7$ are the vertices of the polytope $\mathbf{2_{31}}$. The weights of **56** are the vertices of a Delaunay polytope $\mathbf{3_{21}}$ also called the Hesse polytope by Conway and Sloane.

The Lie algebra of type E_8 has the following decomposition under the maximal subalgebra $\mathrm{E}_7 \oplus A_1$:

$$\mathfrak{e}_8 = (\mathfrak{e}_7 \otimes \mathbf{1}) \oplus (\mathbf{1} \otimes \mathbf{su_2}) \oplus (\mathbf{56} \otimes \mathbf{2}). \tag{3.2}$$

The roots of E_8 are the following 240 vectors of $\mathbb{R}^8$ all located on a seven-dimensional sphere of

radius $\sqrt{2}$:

$$\begin{array}{ll} \frac{1}{2}(\pm 1, \pm 1, \pm 1, \pm 1, \pm 1, \pm 1, \pm 1, \pm 1) & \text{(with an even number of minus signs)} \\ (\pm 1, \pm 1, 0, 0, 0, 0, 0, 0) & \text{(and permutations thereof)} \end{array} \tag{3.3}$$

By definition, the root system E_7 consists of the subsystem of roots of E_8 perpendicular to a chosen root s of E_8. The Weyl group $W(E_8)$ preserves the scalar product (r_1, r_2) between roots. All the roots of E_8 can be organized by their scalar products with respect to the chosen root s of E_8. Since the root system E_8 is crystallographic and simply-laced, the scalar product of two roots can only take one of the following five values: -2, -1, 0, $+1$, $+2$. Then, the following facts are directly proven by using the scalar product:

- There is a unique root r such that $(s, r) = 2$ (resp. -2), namely s (resp. $-s$).
- There are 126 roots perpendicular to s, they form an E_7 root system.
- There are 56 roots r of E_8 with scalar product $(s, r) = 1$ (resp. -1), we call them $\mathbf{56}_+$ (resp. $\mathbf{56}_-$). Each of $\mathbf{56}_\pm$ form a weight system of the irreducible representation $\mathbf{56}$ of E_7.
- Translation by $-s$ gives an isometry between the weight systems $\mathbf{56}_+$ and $\mathbf{56}_-$ corresponding to the hyperplane reflection induced by the root s.
- The involution $r \to -r$ of E_8 exchanges $\mathbf{56}_+$ and $\mathbf{56}_-$.

Using the scalar product of E_8, the weight system $\mathbf{56}_+$ is composed of the closest roots to s. They are all on a sphere of radius $\sqrt{2}$ centered at the affine point P_s defined by the vector s. The roots of E_7 are all on the plane perpendicular to the vector s on a sphere of radius 2 centered at the affine point P_s corresponding to the vector s. The vectors of the weight system $\mathbf{56}_-$ are on a sphere of radius $\sqrt{6}$ centered at the point P_s. The root $-s$ is the further away at a distance $\sqrt{8}$. The root system E_7 defined by $(r, s) = 0$ and the two representations $\mathbf{56}$ are on parallel hyperplanes.

Consider the root $s = (0, 0, 0, 0, 0, 0, 1, 1)$ of E_8. We can write an E_7 root system by listing the roots of E_8 perpendicular to s:

$$\begin{array}{ll} \pm\frac{1}{2}(\pm 1, \pm 1, \pm 1, \pm 1, \pm 1, \pm 1, 1, -1) & \text{(with even number of minus signs)} \\ (\pm 1, \pm 1, 0, 0, 0, 0, 0, 0) & \text{(and permutations of the first six coordinates thereof)} \\ \pm(0, 0, 0, 0, 0, 0, 1, -1) & \end{array} \tag{3.4}$$

We can also determine the weights of the representation $\mathbf{56}$ corresponding to $\mathbf{56}_+$ by enumerating the roots of E_8 with scalar product $+1$ with s:

$$\begin{array}{ll} \frac{1}{2}(\pm 1, \pm 1, \pm 1, \pm 1, \pm 1, \pm 1, 1, 1) & \text{(with even number of minus signs)} \\ (\pm 1, 0, 0, 0, 0, 0, 1, 0) & \text{(and permutations of the first six coordinates thereof)} \\ (\pm 1, 0, 0, 0, 0, 0, 0, 1) & \text{(and permutations of the first six coordinates thereof)} \end{array} \tag{3.5}$$

The opposite of these vectors form the weight system $\mathbf{56}_-$. The representation $\mathbf{56}_\pm$ is invariant under the group $(\mathbb{Z}/2\mathbb{Z})^2$ generated by the involutions $r \mapsto \pm s - r$ and the reflection $\sigma_s : r \to -r + (s, r)s$.

In the basis of fundamental weights, the weights of the representation $\mathbf{56}$ are listed with the corresponding Hasse diagram is given in Figure 3.3.

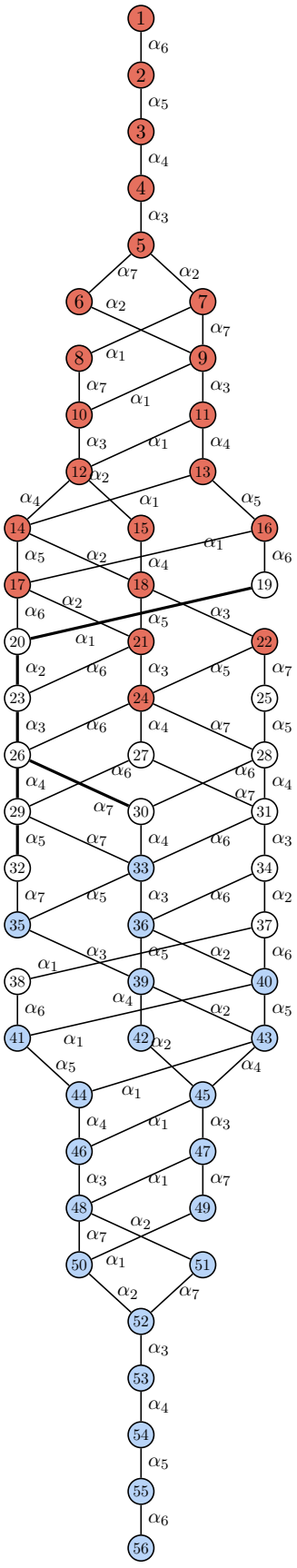

$$
\begin{array}{lc}
\varpi_1 & \begin{bmatrix} 0 & 0 & 0 & 0 & 0 & 1 & 0 \end{bmatrix} \\
\varpi_2 & \begin{bmatrix} 0 & 0 & 0 & 0 & 1 & -1 & 0 \end{bmatrix} \\
\varpi_3 & \begin{bmatrix} 0 & 0 & 0 & 1 & -1 & 0 & 0 \end{bmatrix} \\
\varpi_4 & \begin{bmatrix} 0 & 0 & 1 & -1 & 0 & 0 & 0 \end{bmatrix} \\
\varpi_5 & \begin{bmatrix} 0 & 1 & -1 & 0 & 0 & 0 & 1 \end{bmatrix} \\
\varpi_6 & \begin{bmatrix} 0 & 1 & 0 & 0 & 0 & 0 & -1 \end{bmatrix} \\
\varpi_7 & \begin{bmatrix} 1 & -1 & 0 & 0 & 0 & 0 & 1 \end{bmatrix} \\
\varpi_8 & \begin{bmatrix} -1 & 0 & 0 & 0 & 0 & 0 & 1 \end{bmatrix} \\
\varpi_9 & \begin{bmatrix} 1 & -1 & 1 & 0 & 0 & 0 & -1 \end{bmatrix} \\
\varpi_{10} & \begin{bmatrix} -1 & 0 & 1 & 0 & 0 & 0 & -1 \end{bmatrix} \\
\varpi_{11} & \begin{bmatrix} 1 & 0 & -1 & 1 & 0 & 0 & 0 \end{bmatrix} \\
\varpi_{12} & \begin{bmatrix} -1 & 1 & -1 & 1 & 0 & 0 & 0 \end{bmatrix} \\
\varpi_{13} & \begin{bmatrix} 1 & 0 & 0 & -1 & 1 & 0 & 0 \end{bmatrix} \\
\varpi_{14} & \begin{bmatrix} -1 & 1 & 0 & -1 & 1 & 0 & 0 \end{bmatrix} \\
\varpi_{15} & \begin{bmatrix} 0 & -1 & 0 & 1 & 0 & 0 & 0 \end{bmatrix} \\
\varpi_{16} & \begin{bmatrix} 1 & 0 & 0 & 0 & -1 & 1 & 0 \end{bmatrix} \\
\varpi_{17} & \begin{bmatrix} -1 & 1 & 0 & 0 & -1 & 1 & 0 \end{bmatrix} \\
\varpi_{18} & \begin{bmatrix} 0 & -1 & 1 & -1 & 1 & 0 & 0 \end{bmatrix} \\
\varpi_{19} & \begin{bmatrix} 1 & 0 & 0 & 0 & 0 & -1 & 0 \end{bmatrix} \\
\varpi_{20} & \begin{bmatrix} -1 & 1 & 0 & 0 & 0 & -1 & 0 \end{bmatrix} \\
\varpi_{21} & \begin{bmatrix} 0 & -1 & 1 & 0 & -1 & 1 & 0 \end{bmatrix} \\
\varpi_{22} & \begin{bmatrix} 0 & 0 & -1 & 0 & 1 & 0 & 1 \end{bmatrix} \\
\varpi_{23} & \begin{bmatrix} 0 & -1 & 1 & 0 & 0 & -1 & 0 \end{bmatrix} \\
\varpi_{24} & \begin{bmatrix} 0 & 0 & -1 & 1 & -1 & 1 & 1 \end{bmatrix} \\
\varpi_{25} & \begin{bmatrix} 0 & 0 & 0 & 0 & 1 & 0 & -1 \end{bmatrix} \\
\varpi_{26} & \begin{bmatrix} 0 & 0 & -1 & 1 & 0 & -1 & 1 \end{bmatrix} \\
\varpi_{27} & \begin{bmatrix} 0 & 0 & 0 & -1 & 0 & 1 & 1 \end{bmatrix} \\
\varpi_{28} & \begin{bmatrix} 0 & 0 & 0 & 1 & -1 & 1 & -1 \end{bmatrix}
\end{array}
\qquad
\begin{array}{lc}
\varpi_{29} & \begin{bmatrix} 0 & 0 & 0 & -1 & 1 & -1 & 1 \end{bmatrix} \\
\varpi_{30} & \begin{bmatrix} 0 & 0 & 0 & 1 & 0 & -1 & -1 \end{bmatrix} \\
\varpi_{31} & \begin{bmatrix} 0 & 0 & 1 & -1 & 0 & 1 & -1 \end{bmatrix} \\
\varpi_{32} & \begin{bmatrix} 0 & 0 & 0 & 0 & -1 & 0 & 1 \end{bmatrix} \\
\varpi_{33} & \begin{bmatrix} 0 & 0 & 1 & -1 & 1 & -1 & -1 \end{bmatrix} \\
\varpi_{34} & \begin{bmatrix} 0 & 1 & -1 & 0 & 0 & 1 & 0 \end{bmatrix} \\
\varpi_{35} & \begin{bmatrix} 0 & 0 & 1 & 0 & -1 & 0 & -1 \end{bmatrix} \\
\varpi_{36} & \begin{bmatrix} 0 & 1 & -1 & 0 & 1 & -1 & 0 \end{bmatrix} \\
\varpi_{37} & \begin{bmatrix} 1 & -1 & 0 & 0 & 0 & 1 & 0 \end{bmatrix} \\
\varpi_{38} & \begin{bmatrix} -1 & 0 & 0 & 0 & 0 & 1 & 0 \end{bmatrix} \\
\varpi_{39} & \begin{bmatrix} 0 & 1 & -1 & 1 & -1 & 0 & 0 \end{bmatrix} \\
\varpi_{40} & \begin{bmatrix} 1 & -1 & 0 & 0 & 1 & -1 & 0 \end{bmatrix} \\
\varpi_{41} & \begin{bmatrix} -1 & 0 & 0 & 0 & 1 & -1 & 0 \end{bmatrix} \\
\varpi_{42} & \begin{bmatrix} 0 & 1 & 0 & -1 & 0 & 0 & 0 \end{bmatrix} \\
\varpi_{43} & \begin{bmatrix} 1 & -1 & 0 & 1 & -1 & 0 & 0 \end{bmatrix} \\
\varpi_{44} & \begin{bmatrix} -1 & 0 & 0 & 1 & -1 & 0 & 0 \end{bmatrix} \\
\varpi_{45} & \begin{bmatrix} 1 & -1 & 1 & -1 & 0 & 0 & 0 \end{bmatrix} \\
\varpi_{46} & \begin{bmatrix} -1 & 0 & 1 & -1 & 0 & 0 & 0 \end{bmatrix} \\
\varpi_{47} & \begin{bmatrix} 1 & 0 & -1 & 0 & 0 & 0 & 1 \end{bmatrix} \\
\varpi_{48} & \begin{bmatrix} -1 & 1 & -1 & 0 & 0 & 0 & 1 \end{bmatrix} \\
\varpi_{49} & \begin{bmatrix} 1 & 0 & 0 & 0 & 0 & 0 & -1 \end{bmatrix} \\
\varpi_{50} & \begin{bmatrix} -1 & 1 & 0 & 0 & 0 & 0 & -1 \end{bmatrix} \\
\varpi_{51} & \begin{bmatrix} 0 & -1 & 0 & 0 & 0 & 0 & 1 \end{bmatrix} \\
\varpi_{52} & \begin{bmatrix} 0 & -1 & 1 & 0 & 0 & 0 & -1 \end{bmatrix} \\
\varpi_{53} & \begin{bmatrix} 0 & 0 & -1 & 1 & 0 & 0 & 0 \end{bmatrix} \\
\varpi_{54} & \begin{bmatrix} 0 & 0 & 0 & -1 & 1 & 0 & 0 \end{bmatrix} \\
\varpi_{55} & \begin{bmatrix} 0 & 0 & 0 & 0 & -1 & 1 & 0 \end{bmatrix} \\
\varpi_{56} & \begin{bmatrix} 0 & 0 & 0 & 0 & 0 & -1 & 0 \end{bmatrix}
\end{array}
$$

Figure 3.3: Hasse diagram for the weights of the representation **56** of E_7. The node i represents the weight ϖ_i given above and written in the basis of fundamental weights. A root α between two nodes i and j (with $i < j$) indicates that $\varpi_j = \varpi_i - \alpha$. The white nodes are those corresponding to the weights used to define the sign vector that characterizes the chambers of the hyperplane arrangement I(**56**, E_7). In a given chamber of I(**56**, E_7), each white node takes a specific sign (see section (3.3)). The red (resp. blue) nodes correspond to weights in the positive (resp. negative) conical hull of positive roots. In particular, a white node corresponds to a weight ϖ such that the hyperplane $\varpi^\perp$ intersects the interior of the dual fundamental Weyl chamber while that is not the case for a weight corresponding to a blue or red node.

3.3 Chamber structure of the hyperplane I(E_7,56)

The following Theorem was given in [38] without a formal proof. We give a proof here using the language of sign vectors in the spirit of [22, 23].

Theorem 3.1. *The hyperplane arrangement $I(E_7, \mathbf{56})$ has eight chambers. Each chamber is simplicial. The adjacency graph of the chambers is isomorphic to the Dynkin diagram of type E_8.*

Proof. Since the minuscule representation of E_7 is self-dual, it is enough to consider only half of its weights to study the hyperplane arrangement $I(E_7, \mathbf{56})$. The weights that do not intersect the interior of the dual fundamental Weyl chamber are such that all their coefficients have the same sign when expressed in the basis of simple positive roots. After removing such weights, we are left (up to a sign) with seven weights, listed in Figure 3.4. They have an elegant structure as all can be derived from the smallest one by removing only one root, always different from α_6.

ϖ_{19}	$(1,1,1,\frac{1}{2},0,\text{-}\frac{1}{2},\frac{1}{2})$	1 0 0 0 0 -1 0	ϖ_{19}
ϖ_{20}	$(0,1,1,\frac{1}{2},0,\text{-}\frac{1}{2},\frac{1}{2})$	-1 1 0 0 0 -1 0	$\varpi_{19}-\alpha_1$
ϖ_{23}	$(0,0,1,\frac{1}{2},0,\text{-}\frac{1}{2},\frac{1}{2})$	0 -1 1 0 0 -1 0	$\varpi_{19}-\alpha_1-\alpha_2$
ϖ_{26}	$(0,0,0,\frac{1}{2},0,\text{-}\frac{1}{2},\frac{1}{2})$	0 0 -1 1 0 -1 1	$\varpi_{19}-\alpha_1-\alpha_2-\alpha_3$
ϖ_{29}	$(0,0,0,\text{-}\frac{1}{2},0,\text{-}\frac{1}{2},\frac{1}{2})$	0 0 0 -1 1 -1 1	$\varpi_{19}-\alpha_1-\alpha_2-\alpha_3-\alpha_4$
ϖ_{32}	$(0,0,0,\text{-}\frac{1}{2},\text{-}1,\text{-}\frac{1}{2},\frac{1}{2})$	0 0 0 0 -1 0 1	$\varpi_{19}-\alpha_1-\alpha_2-\alpha_3-\alpha_4-\alpha_5$
ϖ_{30}	$(0,0,0,\frac{1}{2},0,\text{-}\frac{1}{2},\text{-}\frac{1}{2})$	0 0 0 1 0 -1 -1	$\varpi_{19}-\alpha_1-\alpha_2-\alpha_3-\alpha_7$

In the first column, the weights ϖ are written in the basis of simple roots, while in the second column, they are written in the basis of simple fundamental weights. We denote by ϕ an element of the coroot space. When writing ϕ in coordinates, we use the basis of simple coroots. Since, by definition, the simple coroots are dual to the fundamental weights, the scalar product $\varpi \cdot \phi$ is defined using the identity matrix. We define a sign vector for the hyperplane arrangement $I(E_7, \mathbf{56})$ as follows:[3]

$$\phi \mapsto (\varpi_{19}\cdot\phi, \varpi_{20}\cdot\phi, \varpi_{23}\cdot\phi, \varpi_{26}\cdot\phi, \varpi_{29}\cdot\phi, \varpi_{32}\cdot\phi, \varpi_{30}\cdot\phi), \tag{3.6}$$

which gives

$$\begin{aligned}\sigma(\phi) =&(\phi_1-\phi_6, -\phi_1+\phi_2-\phi_6, -\phi_2+\phi_3-\phi_6,\\ &-\phi_3+\phi_4-\phi_6+\phi_7, -\phi_4+\phi_5-\phi_6+\phi_7, -\phi_5+\phi_7, \phi_4-\phi_6-\phi_7).\end{aligned} \tag{3.7}$$

The open dual fundamental Weyl chamber of E_7 is defined as the cone $(\alpha_i \cdot \phi) > 0$ with $i = \{1,2,3,4,5,6,7\}$.

Each chamber is uniquely defined by the signs of entries of the vector $\sigma(\phi)$ when evaluated at any interior point ϕ of the chamber. The weights have a partial order defined by adding positive simple roots: $\varpi_i \succ \varpi_j$ if $\varpi_i - \varpi_j$ is a nonnegative integer linear combination of positive roots. In

[3] Each weight of the representation **56** has norm square 3/2 and has scalar product $\pm 1/2$ with any other weight of **56**. Our choice of signs for the entries of the sign vector is such that the highest weight 0 0 0 0 0 1 0 has a sign $(-1,-1,-1,-1,-1,-1,-1)$.

particular, the partial order for the weights that are interior walls is (see Figure 3.4):

$$\varpi_{19} \succ \varpi_{20} \succ \varpi_{23} \succ \varpi_{26} \succ \varpi_{29} \succ \varpi_{32}, \quad \varpi_{26} \succ \varpi_{30}.$$

Thus, writing the sign vector as in Figure 3.4, we have the following rule:

1. The negative sign flows as the arrows of Figure 3.4.
2. The forms $\varpi_{30} \cdot \phi$ and $\varpi_{29} \cdot \phi$ cannot both be positive at the same time.

For example, if $\varpi_{19} \cdot \phi$ is negative, the same is true of all the $\varpi_i \cdot \phi$ with $i = \{20, 23, 26, 29, 32, 30\}$. The second rule is justified by the fact that $\varpi_{30} + \varpi_{29} = -\alpha_6$ and we are restricted to the dual Weyl chamber. To define a chamber, we just need to name which one of the $\varpi_i \cdot \phi$ is the first negative one with respect to the order given above. If both $\varpi_{26} \cdot \phi$ and $\varpi_{30} \cdot \phi$ are positive, then $\varpi_{19} \cdot \phi$, $\varpi_{20} \cdot \phi$, and $\varpi_{23} \cdot \phi$ are all positive, $\varpi_{29} \cdot \phi$ is necessarily negative (since $\varpi_{30} \cdot \phi$ is positive), which forces $\varpi_{32} \cdot \phi$ to also be negative. There are exactly eight possibilities satisfying these two rules. They are listed in Table 1 and we check explicitly by solving inequalities that they all occur. Their adjacency graph is a Dynkin diagram of type E_8 illustrated in Figure 1.1 where we label the chambers by the corresponding simple roots of E_8. □

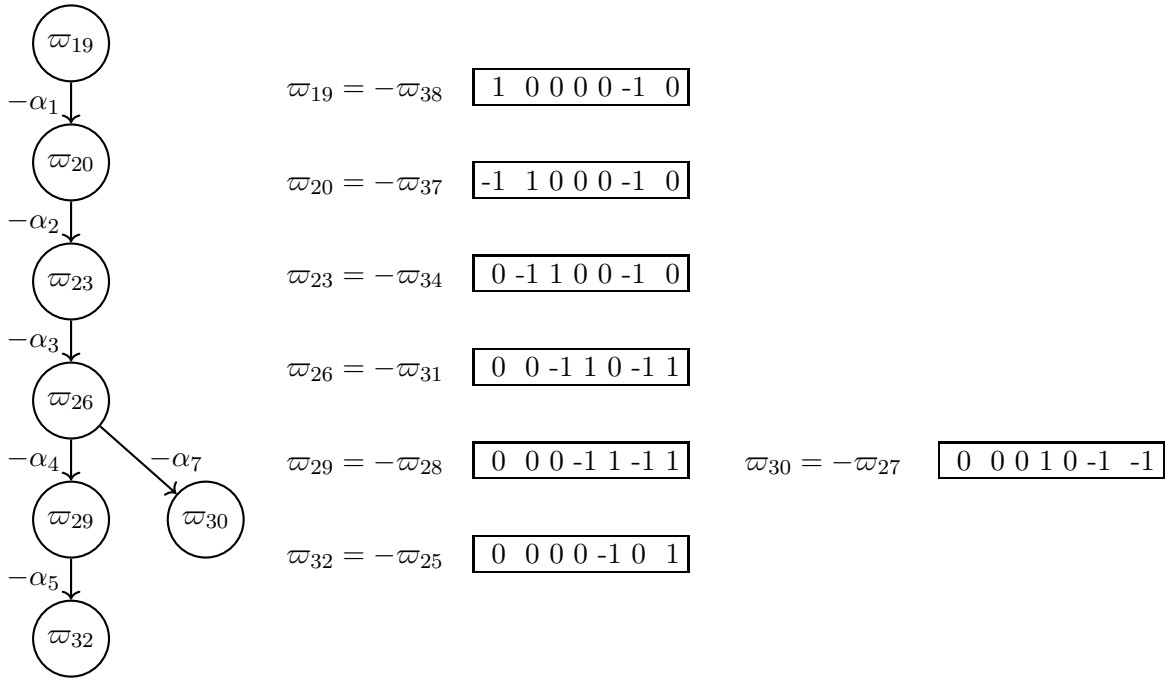

Figure 3.4: Up to a sign, there are seven weights of the representation **56** of E_7 such that each of them has a kernel intersecting the interior of the dual fundamental Weyl chamber. The partial order of weights provide the Hasse diagram presented above and corresponding to a decorated Dynkin diagram of type E_7. We write $\varpi_i \xrightarrow{-\alpha_\ell} \varpi_j$ to indicate that $\varpi_i - \alpha_\ell = \varpi_j$. The linear forms defined by these weights give the sign vector for the hyperplane arrangement $\mathrm{I}(\mathrm{E}_7, \mathbf{56})$.

4 Minimal models Y_4, Y_5, Y_6, and Y_8

In this section, we construct four distinct relative minimal models over the Weierstrass model of an E_7-model as crepant resolutions of the Weierstrass model in equation (1.4). We also study the flops between these distinct crepant resolutions. These relative minimal models correspond to chambers Ch_4, Ch_5, Ch_6, and Ch_8 of the hyperplane arrangement I(E_7, **56**) discussed in section 3.3. Accordingly, we denote these mimimal models by Y_4, Y_5, Y_6, and Y_8. We can tell them apart by identifying the extreme rays of de crepant resolution over the Weierstrass model. To each extreme ray C, we associate a unique weight of the representation **56** of E_7. The identification is given by computing minus the intersection of the curve C with the fibral divisors D_i ($i = 1, \ldots, 7$) not touching the section of the elliptic fibration. The flops between the four minimal models Y_4, Y_5, Y_6, and Y_8 form a Dynkin diagram of type D_4 as illustrated in Figure 1.1.

4.1 Overview of the sequence of blowups defining the resolutions

Each of the models Y_4, Y_5, Y_6, and Y_8 can be obtained by numerous sequences of blowups. We give two distinct resolutions for Y_4 and Y_5 to ease the description of the flops. We will give two trees of blowups defining respectively crepant resolutions of the triples (Y_4, Y_5, Y_8) and (Y_4, Y_6,Y_8). The flops within each of these triples will be modeled by the flops of a suspended pinch point. The graph of flops of a suspended pinch point is a Dynkin diagram of type A_3 and gluing two such Dynkin diagram along two consecutive nodes gives a D_4-Dynkin diagram. For us, the two consecutive nodes will correspond to Y_4 and Y_5 and this explains why we give two distinct resolutions for these two minimal models.

Conventions for blowups. Each crepant resolution is an embedded resolution defined by a sequence of blowups with smooth centers. We denote the blowup $X_{i+1} \to X_i$ along the ideal $(f_1, f_2, \ldots, f_n)$ with exceptional divisor E as:

$$X_i \xleftarrow{(f_1, \ldots, f_n | E)} X_{i+1} \ ,$$

where X_0 is the projective bundle in which the Weierstrass model is defined.

We abuse notations and call the proper transforms of the variables involved in the blowup by the same name. That means for example that we implement $(u_1, \ldots, u_n | e_1)$ by the birational transformation $(u_1, \ldots, u_n) \mapsto (u_1 e_1, \ldots, u_n e_1)$ with the understanding that we introduce at the same time projective coordinates $[u_1 : \ldots : u_n]$ which are the projective coordinates of the fiber of a $\mathbb{P}^{n-1}$-bundle introduced by the blowup. In particular, after the blowup, $(u_1, \ldots, u_n)$ cannot vanish simultaneously as they are projective coordinates of a $\mathbb{P}^{n-1}$. If we blowup a regular sequence $(u_1, \ldots, u_n)$ and the defining equation has multiplicity $n-1$ along $V(u_1, \ldots, u_n)$, then by adjunction, it is easy to see that the embedded blowup defines a crepant map.

The sequence of blowups that we consider for the resolutions Y_4 and Y_5, and to understand the

flops between Y_4, Y_5, and Y_8, are the following

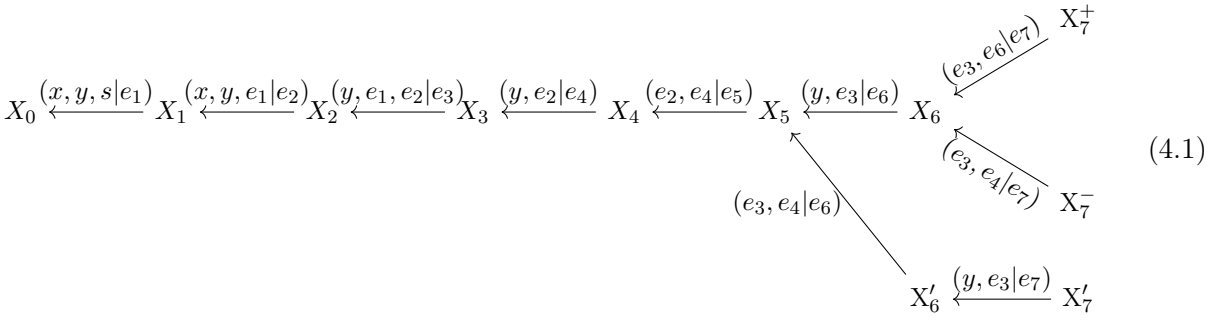

(4.1)

where X_0 is the projective bundle in which the Weierstrass model is defined. We work with embedded resolutions. The minimal models Y_4, Y_5, and Y_8 are obtained as the proper transform of the Weierstrass model in X_7^+, X_7^-, and X_7', respectively.

To understand the flops between Y_4, Y_5, and Y_6, we consider the following tree of blowups:

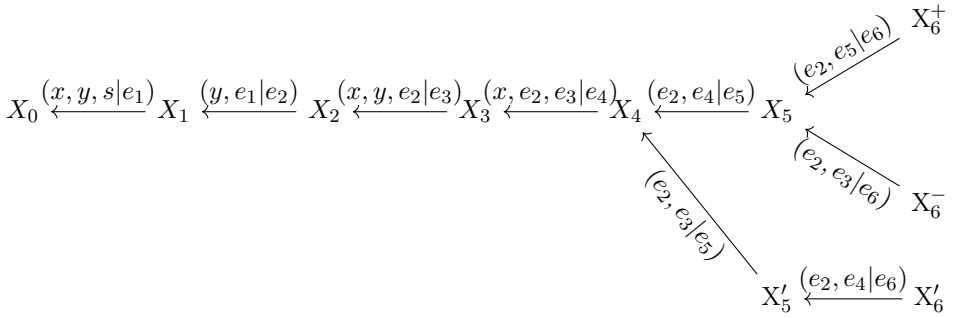

(4.2)

where Y_4, Y_5, and Y_6 are obtained as the proper transform of the Weierstrass model in X_6^+ , X_6^-, and X_6', respectively.

Conventions for Cartan divisors and fibers. We denote the fibral divisors by D_m where $m = 0, 1, \ldots, 7$ and D_0 is the divisor touching the zero section of the elliptic fibration. By definition, each D_m is a fibration of a rational curve over the divisor S in the base. We denote the generic curve of D_m by C_m. The intersection numbers $\int_Y D_m \cdot C_n$ are minus the Cartan matrix of the affine Dynkin diagram of type $\widetilde{\mathrm{E}}_7$. The fibral divisors not touching the section are denoted D_i with $i = 1, 2, \ldots, 7$. We recall that the weight of a vertical curve C is by definition the vector of minus its intersection number with the fibral divisors:

$$(-\int_Y D_0 \cdot C, -\int_Y D_1 \cdot C, \ldots, -\int_Y D_7 \cdot C).$$

They are not independent, as the linear combination with coefficients $(1, 2, 3, 4, 3, 2, 1, 2)$ gives zero.[4] For that reason, it is enough to compute only the intersection with the D_i, which gives a vector in the weight lattice of E_7.

[4]These coefficients are the multiplicities of the node of the fiber III* and also correspond to the Dynkin labels of the highest root of E_7 with one given for the extra node.

4.2 The geometry of Y_4

We study the minimal model Y_4 using the resolution discussed in equation (4.1). Y_4 is then the proper transform of the Weierstrass model of equation (1.4) after the blowups leading to X_7^+ in equation (4.1). The result is:

$$\mathrm{Y}_4: \quad e_4e_6y^2 - e_1e_2e_3(e_2e_4e_5^2x^3 + ae_1s^3x + be_1^2e_3e_6e_7^2s^5) = 0. \tag{4.3}$$

The relative projective coordinates are:

$$\begin{array}{c}[e_2e_3e_4e_5^2e_6e_7^2x : e_2e_3^2e_4^2e_5^3e_6^3e_7^5y : s][x : e_3e_4e_5e_6^2e_7^3y : e_1e_3e_6e_7^2]\\ [e_4e_5e_6e_7y : e_1 : e_2e_4e_5^2][e_6e_7y : e_2e_5][e_2 : e_4][y : e_3e_7][e_3 : e_6].\end{array} \tag{4.4}$$

The divisor for the special fiber is $se_1e_2e_3^2e_4e_5^2e_6^2e_7^4$. The fibral divisors are:

$$\begin{cases} 1\ D_0: & s = e_6y^2 - e_1e_2^2e_3e_5^2x^3 = 0\\ 2\ D_1: & e_1 = y = 0\\ 3\ D_2: & e_1 = e_6 = 0\\ 4\ D_3: & e_7 = e_4e_6y^2 - e_1e_2^2e_3e_4e_5^2x^3 - ae_1^2e_2e_3s^3x = 0\\ 3\ D_4: & e_3 = e_4 = 0\\ 2\ D_5: & e_1 = e_4 = 0\\ 1\ D_6: & e_4 = be_1e_3e_6e_7^2s^2 + ax = 0\\ 2\ D_7: & e_6 = e_2e_4e_5^2x^2 + ae_1s^3 = 0 \end{cases} \tag{4.5}$$

We denote by C_a the generic fiber of the fibral divisor D_a. All the fibral divisors are $\mathbb{P}^1$-bundles with the exception of D_3 and D_6.

Remark 4.1. One might think that the curve C_7 degenerates at $a = 0$. However, that is not the case because when $a = 0$, the defining equation for C_7 gives $e_6 = e_2e_4e_5^2x^2 = 0$. Since e_6 and e_2e_4x cannot vanish simultaneously, as is clear by looking at the projective coordinates, we deduce that over $V(a) \cap S$, the curve C_7 simplifies to $C_7 : a = e_6 = e_4 = 0$ but does not degenerate. It follows that D_0, D_1, D_2, D_4, and D_5 are $\mathbb{P}^1$-projective bundles.

The degeneration at $a = 0$ gives:

$$\begin{cases} C_3 \longrightarrow C_{36} + C_3', \\ C_6 \longrightarrow 2C_{36} + C_7 + C_4, \end{cases} \tag{4.6}$$

where

$$C_3': \quad a = e_7 = e_6y^2 - e_1e_2^2e_3e_5^2x^3 = 0, \quad C_{36}: \ a = e_4 = e_7 = 0. \tag{4.7}$$

Only C_{36} and C_3' are new rational curves produced by the degeneration at $V(s, a)$. They are extreme

rays. The geometric weights of these curves are:

$$\begin{cases} C_{36} = \frac{1}{2}(C_6 - C_4 - C_7) \to \boxed{\text{0 0 0 -1 1 0 -1 1}} = \varpi_{26}, \\ C_3' = \frac{1}{2}(2C_3 - C_6 + C_4 + C_7) \to \boxed{\text{0 0 1 -1 0 0 1 0}} = -\varpi_{23}. \end{cases} \tag{4.8}$$

The two weights ϖ_{26} and ϖ_{23} are weights of the representation **56** and uniquely characterize the chamber Ch_4 of the hyperplane arrangement I(E_7,**56**).

Taking into account the multiplicities of the curves C_4, C_6, and C_7, we have

$$4C_3 + C_6 \longrightarrow 6C_{36} + 4C_3' + C_4 + C_7. \tag{4.9}$$

Together with the remaining curves, we get a fiber of type II* (with dual fiber the affine Dynkin diagram $\widetilde{\mathrm{E}}_8$) but with the node of multiplicity 5 (the node α_4 of $\widetilde{\mathrm{E}}_8$) contracted to a point as illustrated on Figure 4.1.

Remark 4.2. We also note that the fiber C_6 over $V(s, a, b)$ jumps in dimension and becomes a quadric surface. Thus the resolution of the E_7-fiber does not give a flat elliptic fibration when the base is a threefold and a and b can vanish simultaneously on S. No other fiber component jumps in dimension.

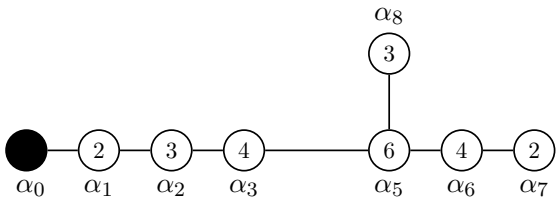

Figure 4.1: The resolution in Chamber 4 has a fiber $\tilde{\mathrm{E}}_7$ that degenerates to a fiber of type II* with the node α_4 contracted to a point.

4.3 The geometry of Y_5

We study the minimal model Y_5 using the resolution discussed in equation (4.1). Y_5 is the proper transform of the Weierstrass model of equation (1.4) after the blowups leading to X_7^- in equation (4.1). The result is:

$$Y_5: \quad e_4e_6y^2 = e_1e_2e_3(e_2e_4e_5^2e_7x^3 + ae_1s^3x + be_1^2e_3e_6e_7s^5). \tag{4.10}$$

The relative projective coordinates due to the successive blowups are

$$\begin{gathered} [e_2e_3e_4e_5^2e_6e_7^2x : e_2e_3^2e_4^2e_5^3e_6^3e_7^4y : s][x : e_3e_4e_5e_6^2e_7^2y : e_1e_3e_6e_7] \\ [e_4e_5e_6e_7y : e_1 : e_2e_4e_5^2e_7][e_6y : e_2e_5][e_2 : e_4e_7][y : e_3e_7][e_3 : e_4]. \end{gathered} \tag{4.11}$$

The divisor for the special fiber is $se_1e_2e_3^2e_4e_5^2e_6^2e_7^3$ with irreducible components:

$$\begin{cases} 1\ D_0: & s = e_1e_2^2e_3e_5^2e_7x^3 - e_6y^2 = 0 \\ 2\ D_1: & e_1 = y = 0 \\ 3\ D_2: & e_1 = e_6 = 0 \\ 4\ D_3: & e_3 = e_6 = 0 \\ 3\ D_4: & e_7 = e_4e_6y^2 - ae_1^2e_2e_3s^3x = 0 \\ 2\ D_5: & e_5 = e_4e_6y^2 - ae_1^2e_2e_3s^3x - be_1^3e_2e_3^2e_6e_7s^5 = 0 \\ 1\ D_6: & e_4 = ax + be_1e_3e_6e_7s^2 = 0 \\ 2\ D_7: & e_6 = e_2e_4e_5^2e_7x^2 + ae_1s^3 = 0 \end{cases} \tag{4.12}$$

All the fibral divisors are $\mathbb{P}^1$-bundles except for D_4, D_6 and D_7 which degenerate over $V(s,a)$:

$$\begin{cases} C_4 \longrightarrow C_{46} + C_{47}, \\ C_6 \longrightarrow C_{46} + C_{67}, \\ C_7 \longrightarrow C_{47} + C_{67} \end{cases} \tag{4.13}$$

where:

$$C_{46}: \quad a = e_4 = e_7 = 0, \quad C_{47}: \quad a = e_6 = e_7 = 0, \quad C_{67}: \quad a = e_4 = e_6 = 0. \tag{4.14}$$

The naming is chosen to reflect the intersection of the original curves rather than our choice of blowup (over a point of $V(s,a)$, C_{ij} is the intersection of D_i and D_j). Taking into account the multiplicities of the curves C_4, C_6, and C_7, we have

$$3C_4 + 2C_7 + C_6 \longrightarrow 5C_{47} + 4C_{46} + 3C_{67}. \tag{4.15}$$

The three new curves (C_{46}, C_{47}, and C_{67}) all intersect at the same point $a = e_4 = e_6 = e_7 = 0$. The curve C_{67} does not intersect any other curves since C_{67} is only visible in the patch $e_5e_3e_2xs \neq 0$. The curve C_{47} intersects transversally the curve C_3 and the curve C_{46} intersects transversally the curve C_5. Altogether, the curves form a fiber of type II* with the nodes of multiplicity 6 (α_5) contracted to a point as illustrated in Figure 4.2.

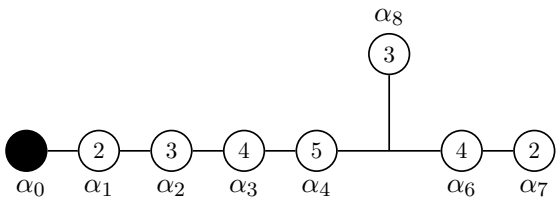

Figure 4.2: The resolution Y_5 (corresponding to Chamber 5) has a fiber $\widetilde{E}_7$ that degenerates to a fiber of type II* (with dual graph $\widetilde{E}_8$) with the node α_4 contracted to a point.

The corresponding weights are

$$\begin{cases} C_{46} = \frac{1}{2}(C_4 + C_6 - C_7) \to \boxed{\text{0 0 0 0 -1 1 -1 1}} = \varpi_{29}, \\ C_{47} = \frac{1}{2}(C_4 + C_7 - C_6) \to \boxed{\text{0 0 0 1 -1 0 1 -1}} = -\varpi_{26}, \\ C_{67} = \frac{1}{2}(C_6 + C_7 - C_4) \to \boxed{\text{0 0 0 0 1 0 -1 -1}} = \varpi_{30}. \end{cases} \tag{4.16}$$

After removing the first component (corresponding to C_0), these vectors become weights in the representation **56** of E_7. The Weyl orbit of each of these weights produces the full representation **56** of E_7 since it is a minuscule representation. The hyperplanes $\varpi_{26}^{\perp}$, $\varpi_{29}^{\perp}$, $\varpi_{30}^{\perp}$ are the interior walls of the chamber Ch_5 (see Figure 1.1). As in Remark 4.2, the node C_6 becomes a rational surface over $V(s,a,b)$.

4.4 The geometry of Y_6

The minimal model Y_6 is discussed using the resolution in (4.2). The proper transform is

$$Y_6: \quad e_2e_3e_5y^2 - e_1(e_3e_6e_4^2x^3 + ae_1e_2s^3x + be_1^2e_2^2e_5e_6s^5) = 0. \tag{4.17}$$

The projective coordinates are

$$\begin{aligned}[e_3e_4^2e_5e_6^2x : e_2e_3^2e_4^3e_5^3e_6^4y : s][e_3e_4e_5e_6y : e_1][e_4e_6x : y : e_2e_4e_5e_6^2][x : e_2e_5e_6 : e_3e_5] \\ [e_2e_6 : e_3][e_2 : e_4].\end{aligned} \tag{4.18}$$

The total transform of s is $se_1e_2e_3e_4^2e_5^2e_6^3$ and the fibral divisors are:

$$\begin{cases} 1\ D_0: & s = e_2e_5y^2 - e_1e_6e_4^2x^3 = 0 \\ 2\ D_1: & e_1 = e_2 = 0 \\ 3\ D_2: & e_2 = x = 0 \\ 4\ D_3: & e_2 = e_6 = 0 \\ 3\ D_4: & e_6 = e_3e_5y^2 - ae_1^2s^3x = 0 \\ 2\ D_5: & e_4 = e_3e_5y^2 - e_1^2s^3(ax + be_1e_2e_5e_6s^2) = 0 \\ 1\ D_6: & e_3 = ax + be_1e_2e_5e_6s^2 = 0 \\ 2\ D_7: & e_5 = e_3e_4^2e_6x^2 + ae_1e_2s^3 = 0 \end{cases} \tag{4.19}$$

The resolution Y_6 (corresponding to Chamber 6) has a fiber III* (with dual graph $\widetilde{\mathrm{E}}_7$) over the generic point of S. But over $V(s,a)$, the fiber III* degenerates as follows:

$$\begin{cases} C_5 \longrightarrow C_{57} + C_5', \\ C_7 \longrightarrow C_4 + C_6 + 2C_{57}. \end{cases} \tag{4.20}$$

We have

$$2C_5 + 2C_7 \longrightarrow 2C_4 + 6C_{57} + 2C_5' + 2C_6, \tag{4.21}$$

where

$$C_{57} : a = e_4 = e_5 = 0, \quad C_5' : e_4 = e_3 y^2 - b e_1^3 e_2 e_6 s^5 = 0. \tag{4.22}$$

The resulting fiber is a fiber of type II* (with dual graph $\widetilde{\mathrm{E}}_8$) with the node α_6 contracted to a point as illustrated in Figure 4.3. The weights of these curves can be computed as follows

$$\begin{cases} C_{57} = \frac{1}{2}(C_7 - C_4 - C_6) \to \boxed{0\ 0\ 0\ 1\ \text{-}1\ 1\ \text{-}1\ 0} = -\varpi_{29}, \\ C_5' = \frac{1}{2}(2C_5 - C_7 + C_4 + C_6) \to \boxed{0\ 0\ 0\ 0\ 0\ \text{-}1\ 0\ 1} = \varpi_{32}. \end{cases} \tag{4.23}$$

These are weights of the representation **56** of E_7. The hyperplanes $\varpi_{29}^{\perp}$ and $\varpi_{32}^{\perp}$ are walls of the chamber Ch_6 of the hyperplane arrangement I(E_7, **56**).

As for Y_4 and Y_5, when the base has at least dimension three, the curve C_6 becomes a quadric surface over $V(s, a, b)$.

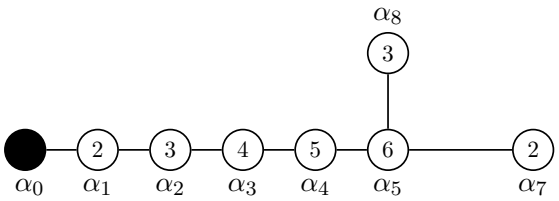

Figure 4.3: The resolution in Chamber 6 has a fiber $\widetilde{\mathrm{E}}_7$ that degenerates to a fiber of type II* with the node α_6 contracted to a point.

4.5 The geometry of Y_8

We study the minimal model Y_8 using the resolution discussed in equation (4.1). Y_5 is the proper transform of the Weierstrass model of equation (1.4) after the blowups leading to X_7^- in equation (4.1). The result is:

$$Y_8 : \qquad e_4 e_7 y^2 - e_1 e_2 e_3 (e_2 e_4 e_5^2 e_6 x^3 + a e_1 s^3 x + b e_1^2 e_3 e_6 e_7 s^5) = 0. \tag{4.24}$$

where the relative projective coordinates are

$$\begin{gathered} [e_2 e_3 e_4 e_5^2 e_6^2 e_7 x : e_2 e_3^2 e_4^2 e_5^3 e_6^4 e_7^3 y : s]\ [x : e_3 e_4 e_5 e_6^2 e_7^2 y : e_1 e_3 e_6 e_7] \\ [e_4 e_5 e_6 e_7 y : e_1 : e_2 e_4 e_5^2 e_6]\ [e_7 y : e_2 e_5]\ [e_2 : e_4 e_6]\ [e_4 : e_3 e_7]\ [y : e_3]. \end{gathered} \tag{4.25}$$

The total transform of s is $se_1e_2e_3^2e_4e_5^2e_6^3e_7^2$ and we have the following fibral divisors

$$\begin{cases} 1\ D_0: & s = e_1e_2^2e_3e_5^2e_6x^3 - e_7y^2 = 0 \\ 2\ D_1: & e_1 = y = 0 \\ 3\ D_2: & e_1 = e_7 = 0 \\ 4\ D_3: & e_3 = e_7 = 0 \\ 3\ D_4: & e_6 = e_4e_7y^2 - ae_1^2e_2e_3s^3x = 0 \\ 2\ D_5: & e_5 = e_4e_7y^2 - ae_1^2e_2e_3s^3x - be_1^3e_2e_3^2e_6e_7s^5 = 0 \\ 1\ D_6: & e_4 = ax + be_1e_3e_6e_7s^2 = 0 \\ 2\ D_7: & e_7 = e_2e_4e_5^2e_6x^2 + ae_1s^3 = 0 \end{cases} \tag{4.26}$$

At $V(s,a)$, we have:

$$C_4 \longrightarrow C_6 + C_7 + 2C_4', \tag{4.27}$$

where

$$C_4' : a = e_6 = y = 0. \tag{4.28}$$

Only C_4' contributes a weight that is not in the root lattice:

$$C_4' \longrightarrow \frac{1}{2}(C_4 - C_6 - C_7) \longrightarrow \boxed{0\ \ 0\,0\,0\ \ -1\,0\,1\,1} = -\varpi_{30}. \tag{4.29}$$

The weight ϖ_{30} is in the representation **56** of E_7. The hyperplane $\varpi_{30}^{\perp}$ perpendicular to ϖ_{30} is the interior wall of chamber Ch_8 of the hyperplane arrangement I(E_7,**56**). The fiber obtained at the degeneration $V(s,a)$ is a one-chain with the following multiplicities:

$$C_0 - 2C_1 - 3C_2 - 4C_3 - 5C_{47} - 6C_4' - 4C_{46} - 2C_5. \tag{4.30}$$

This chain corresponds to an affine Dynkin diagram of type $\tilde{\mathrm{E}}_8$ with the node α_8 removed as illustrated on Figure 4.4.

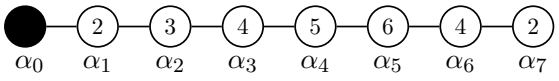

Figure 4.4: The resolution in Chamber 8 has a fiber $\widetilde{\mathrm{E}}_7$ that degenerates to a fiber of type II* with the node α_8 contracted to a point.

4.6 SPP (suspended pinch point) flops

Binomial hypersurfaces are simple algebraic varieties. They can be instrumental in our understanding of flops between minimal models over a Weierstrass model. For example, the binomial variety in $\mathbb{C}^5$ defined by the hypersurface

$$u_1u_2 - w_1w_2w_3 = 0,$$

has six crepant resolutions whose graph of flops is a hexagon (an affine Dynkin diagram of type $\widetilde{\mathrm{A}}_5$). The flop diagram of this binomial variety matches those of the Spin(8)-model [24] and also defines the hexagon of flops of the SU(5) model [35].

The *pinch point* (also called the *Whitney umbrella*) is the singular surface defined by the following binomial equation in $\mathbb{C}^3$:

$$x^2 - y^2 z = 0.$$

The Whitney umbrella is not a normal surface as it has singularities in codimension-one. The Whitney umbrella plays an important role in the geometry of weak coupling limits [1, 2, 15, 32].

The suspended pinch point appears in other areas of string geometry [46]. The *suspended pinch point* is a threefold defined as the double cover of $\mathbb{C}^3$ branched along a Whitney umbrella. Its defining equation in $\mathbb{C}^4$ is

$$u^2 = x^2 - y^2 z.$$

After a change of variables $(u, x, y, z) \to (u_1 = z, u_2 = u + x, u_3 = u - x, u_4 = y)$, the suspended pinch point becomes the following binomial hypersurface in $\mathbb{C}^4$:

$$Z_0 : u_1 u_4^2 = u_2 u_3.$$

The singularities of the suspended pinch point are in codimension-two, more precisely, the singular locus is the line $u_2 = u_3 = u_4 = 0$ and the singularity worsens at the origin. The variety is normal and has three distinct crepant resolutions whose graph of flops is a Dynkin diagram of type A_3. The three crepant resolutions of the suspended pinch points are presented algebraically in Figure 4.5. We also give a toric description of all the crepant partial resolutions in Figure 4.6. The algebraic crepant resolutions given in Figure 4.5 should be compared to the right tails of the trees of resolutions presented in equations (4.1) and (4.2). This explains why the flops between the minimal models Y_4, Y_5, Y_6, and Y_8 are inspired by those of the suspended pinch point.

Blowing up (u_1, u_2) by $(u_1, u_2) \to (r_1 \tilde{u}_1, r_1 \tilde{u}_2)$ with exceptional divisor $r_1 = 0$, the proper transform of Z_0 is

$$\tilde{Z}_0 : \tilde{u}_2 u_3 - \tilde{u}_1 u_4^2 = 0.$$

The variables $[\tilde{u}_1 : \tilde{u}_2]$ are the projective coordinates of a $\mathbb{P}^1$, in particular, $\tilde{u}_1$ and $\tilde{u}_2$ cannot vanish at the same time. It follows that $\tilde{Z}_0$ is singular at $u_4 = \tilde{u}_2 = u_3 = 0$, which is defined in the patch $\tilde{u}_1 \neq 0$. In that patch, $\tilde{Z}_0$ is isomorphic to the cylindrical quadric cone

$$(\mathbb{C}^2/\mathbb{Z}_2) \times \mathbb{C},$$

where the $\mathbb{Z}_2$ involution is generated by minus the identity of $\mathbb{C}^2$. As a hypersurface in $\mathbb{C}^4$, it is given by the zero locus of

$$x^2 - yz = 0,$$

where $\mathbb{C}^4$ is parametrized by $(r_1, x = u_4, y = \frac{\tilde{u}_2}{\tilde{u}_1}, z = u_3)$. This cone has a unique crepant resolution obtained, for example, by blowing up (x, y). For $\tilde{Z}_0$, we blowup (u_4, u_2) using the birational map $(u_4, u_2) \to (\tilde{u}_4 r_2, \tilde{u}_2 r_2)$, where $r_2 = 0$ is the exceptional divisor. The proper transform is the crepant

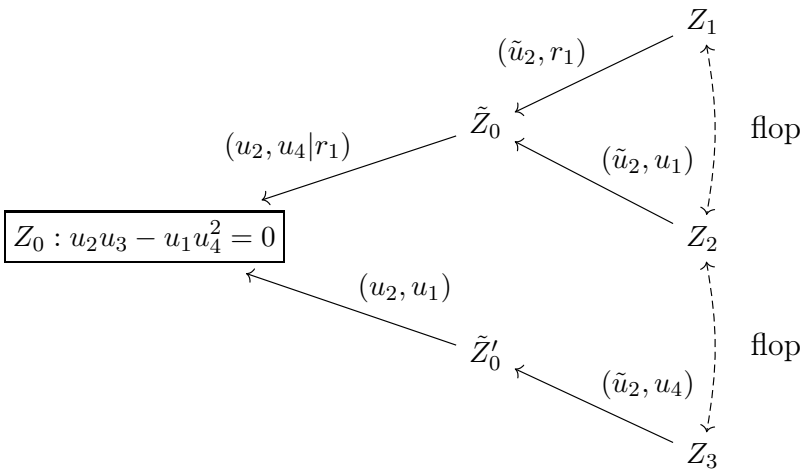

Figure 4.5: The three crepant resolutions of the suspended pinch point $Z_0 : u_2u_3 - u_1u_4^2 = 0$. In the blowup defining Z_1, $r_1 = 0$ is the exceptional locus of the previous blowup defining $\tilde{Z}_0$, i.e. r_1 is the exceptional locus of the blowup of Z_0 centered at $u_2 = u_4 = 0$. The flops between Z_1, Z_2, and Z_3 defines a Dynkin diagram of type A_3 and are all Atiyah flops as shown in Figure 4.6.

resolution

$$Z_3 : r_2\tilde{u}_1\tilde{u}_4^2 - \tilde{u}_2'u_3 = 0.$$

We get the other two crepant resolutions of Z_0 by first blowing up (u_2, u_4) with the birational map $(u_4, u_2) \to (\tilde{u}_4 r_1, \tilde{u}_2 r_1)$, which gives the proper transform

$$\tilde{Z}_0' : u_1r_1\tilde{u}_4^2 - \tilde{u}_2u_3 = 0.$$

The variables $[\tilde{u}_4 : \tilde{u}_2]$ are the projective coordinates of a $\mathbb{P}^1$, in particular, $\tilde{u}_4$ and $\tilde{u}_2$ cannot vanish at the same time. The singular locus of Z_0' is $u_1 = r_1 = u_2 = u_3 = 0$. This singularity is defined in the patch $\tilde{u}_4 \neq 0$ and is a quadric cone

$$k[x, y, z, t]/(xy - zt),$$

where $x = u_1$, $y = r_1$, $z = \tilde{u}_2/\tilde{u}_4$, and $\tilde{u}_3\tilde{u}_4$. Such a quadric cone has two crepant resolutions connected by an Atiyah flop and obtained by blowing up (x, z) and (x, t), respectively. For $\tilde{Z}_0'$, we obtain the two crepant resolutions Z_1 and Z_2 by blowing up $\tilde{Z}_0'$ at $(\tilde{u}_2, r_1)$ and $(\tilde{u}_2, u_1)$, respectively.

The suspended pinch point can also be described as a particular partial resolution of the $\mathbb{Z}_2 \times \mathbb{Z}_2$ orbifold quotient of $\mathbb{C}^3$ [46]:

$$\mathbb{C}^3/(\mathbb{Z}_2 \times \mathbb{Z}_2) : \quad u_4^2 - u_1u_2u_3 = 0.$$

where the Klein group $\mathbb{Z}_2 \times \mathbb{Z}_2$ is generated by the two involution $(z_1, z_2, z_3) \mapsto (-z_1, -z_2, z_3)$ and $(z_1, z_2, z_3) \mapsto (z_1, -z_2, -z_3)$. Consider the blowup centered at (u_4, u_1). In one patch, we have $(u_4, u_1) \to (u_4u_1, u_1)$ which gives the proper transform $u_1u_4^2 = u_2u_3$. The diagram of flops of the crepant resolutions of this orbifold is also a D_4-Dynkin diagram as seen in Figure 4.7.

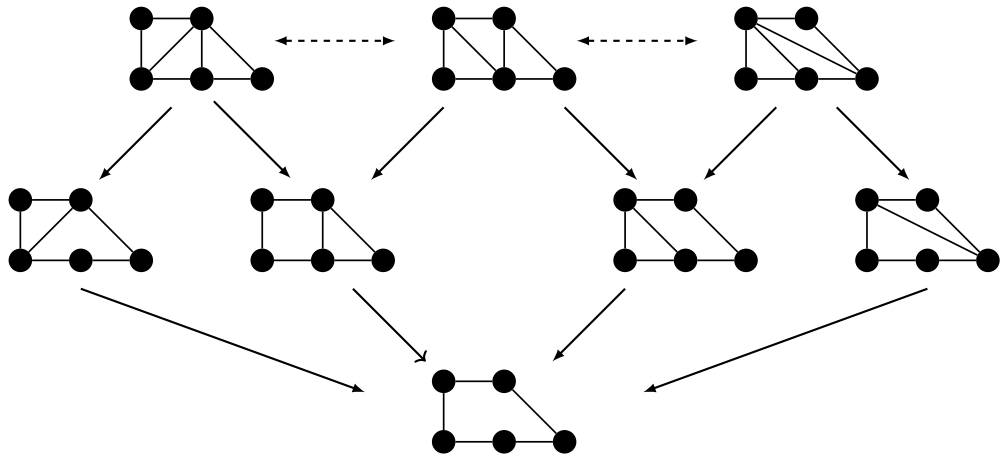

Figure 4.6: Flops between the three crepant resolutions of the suspended pinch point $zu^2 = xy$ and all its toric partial resolutions. The suspended pinch point is at the bottom row. The three crepant resolutions are on the top row. The four partial resolutions are in the middle row. The external varieties of the middle row have the singularities of a cylindrical quadric cone $k[x, y, z, t]/(z^2 - xy)$ while the others have singularities of a quadric threefold with a double point $k[x, y, z, t]/(xy - zt)$.

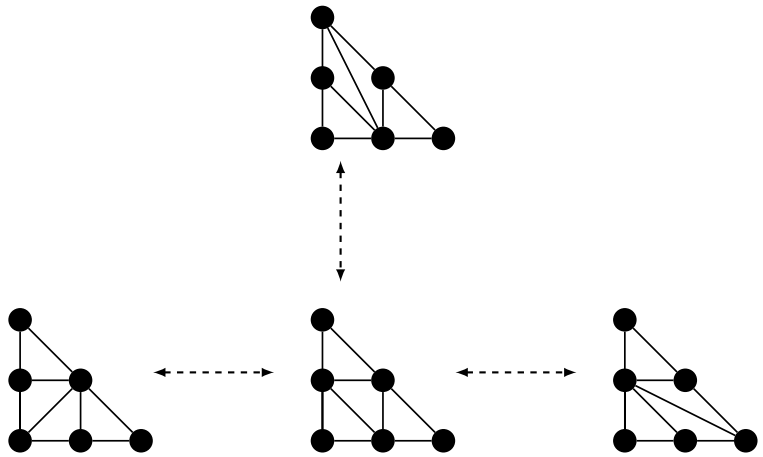

Figure 4.7: Flops between the four crepant resolutions of the singularity $k[x, y, z, t]/(t^2 - xyz)$. This binomial variety is the double cover of $\mathbb{A}^3$ branched along the three coordinate axes. This singular variety is a $\mathbb{Z}_2 \times \mathbb{Z}_2$ orbifold of $\mathbb{C}^3$.

$z^2 = u_1u_2u_3$ (a) $\mathbb{C}^3/(\mathbb{Z}_2 \times \mathbb{Z}_2)$ $u_1u_4^2 = u_2u_3$ (b) Suspended pinch point $u_1u_2 - u_3u_4 = 0$ (c) Double point in $\mathbb{C}^4$ $z^2 = xy$ (d) Quadric cone in $\mathbb{C}^3$

Figure 4.8: Some of the singular binomial varieties encountered in this paper.

4.7 SPP flopping between Y_4, Y_5, Y_6, and Y_8

The flops connecting Y_4, Y_5, and Y_6 can be easily understood using the tree of blowups given in equation (4.2). Consider the proper transform Y of the Weierstrass equation after the four blowups defining X_4 in equation (4.2). By definition, Y is a common blowdown of Y_4, Y_5, and Y_6. It can be written in the following suggestive form (see equation (4.17)):

$$Y: \quad e_2(e_3y^2 - ae_1s^3x + be_1^2e_2^2s^5) - e_3e_4^2(e_1x^3) = 0. \tag{4.31}$$

In the patch $e_1xys \neq 0$, it has the following structure

$$Y: \quad e_2q = e_3e_4^2, \quad q = (e_3y^2 - ae_1s^3x + be_1^2e_2^2s^5)/(e_1x^3). \tag{4.32}$$

We recognize this as a suspended pinch point singularity at the origin $e_2 = q = e_3 = e_4 = 0$. Such a singularity admits three crepant resolutions described by the tail of the tree of blowups in (4.2) and mimic the blowups in Figure 4.5.

The same story hold for the flops between the minimal models Y_8, Y_5, and Y_4 by considering the proper transform of the Weierstrass model after the first five blowups defined in the tree of equation (4.1). After these five blowups, the proper transform of the Weierstrass model of an E_7-model takes the following form (see equation (4.24):

$$e_4y^2 - e_1e_2e_3(e_2e_4e_5^2x^3 + ae_1s^3x + be_1^2e_3s^5) = 0. \tag{4.33}$$

Since when $e_4 = y = 0$, e_1e_2 is nonzero by the projective coordinates in equation (4.25). Thus, we again have an equation of the form

$$e_4y^2 = e_3A. \tag{4.34}$$

We recognize the form of the binomial variety of a suspended pinch point. We then derive Y_4, Y_5, and Y_5 as its three crepant resolutions following the discussion of section 4.6. The last three blowups in each branch of the tree presented in equation (4.1) mimic the resolutions of the suspended pinch points as given in section 4.6.

5 Application to $\mathcal{N} = 1$ five-dimensional theories

M-theory compactified on a Calabi-Yau threefold results in a five-dimensional supersymmetric gauge theory with eight supercharges that we denote $\mathcal{N} = 1$ five-dimensional supergravity. Such a theory contains a gravitational multiplet, n_T tensor multiplets, n_V vector multiplets, and n_H hypermultiplets. In five-dimensional spacetime, a massless tensor multiplet is dual to a massless vector. In what follows, we assume that all tensors are massless and are dualized to vectors. Each vector multiplet contains a real scalar field ϕ and each hypermultiplet contains a quaternion (four real fields). The kinetic terms of all the vector multiplets and the graviphoton as well as the Chern-Simons terms are determined by a real function of the scalar fields called the prepotential $\mathscr{F}(\phi)$.

In the Coulomb branch of an $\mathcal{N} = 1$ supergravity theory in five dimensions, the scalar fields of the vector multiplets take values in the Cartan sub-algebra of the Lie algebra and the Lie group is broken

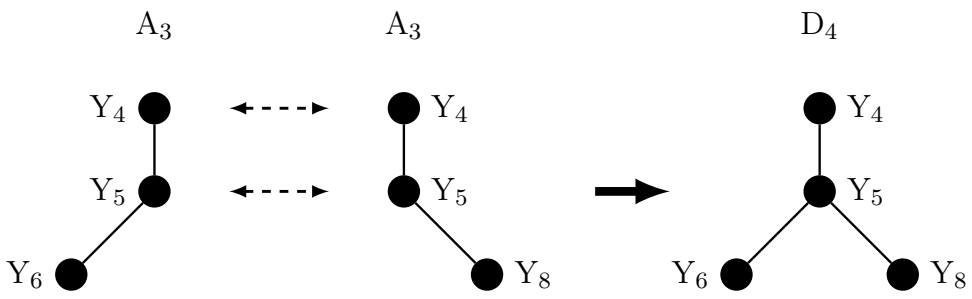

Figure 4.9: The triples (Y_4, Y_5, Y_8) and (Y_4, Y_5, Y_6) both form an A_3 Dynkin diagram where the nodes are the varieties and two nodes are connected if they are related by a flop as shown on the left and middle pictures. For each of the triples, the flops mirror those of a suspended pinch point. By identifying Y_4 and Y_5 of the two triples with themselves, we end up gluing the two A_3 to form a D_4 Dynkin diagram representing all the flops between Y_4, Y_5, Y_6, and Y_8.

to a product of Abelian factors. This implies that the charge of a hypermultiplet is simply a weight of the representation under which it transforms [39]. In the presence of hypermultiplets charged under a representation $\mathbf{R}$ of the gauge group, the Coulomb phase of the theory is characterized by a one-loop quantum correction to the superpotential derived by integrating out massive hypermultiplets. The full quantum superpotential $\mathcal{F}(\varphi)$ is protected from further corrections by supersymmetry and is a piecewise cubic polynomial of the scalar fields. The metric of the scalar fields of the vector multiplets is the matrix of second derivatives of $\mathcal{F}(\varphi)$ and it is differentiable in open regions that define distinct Coulomb branches separated by walls on which some of the massive hypermultiplets become massless and should be added to the low energy description of the theory. The Intrilligator-Morrison-Seiberg (IMS) prepotential is the quantum contribution to the prepotential of a five-dimensional gauge theory after integrating out all massive fields.

Let ϕ be in the Cartan subalgebra of a Lie algebra $\mathfrak{g}$. We denote by $\mathbf{R}_i$ the representations under which the hypermultiplets transform. The weights are in the dual space of the Cartan subalgebra. We denote the evaluation of a weight on a coroot vector ϕ as a scalar product $\langle \mu, \phi \rangle$. Denoting the roots by α and the weights of $\mathbf{R}_i$ by ϖ we have [39]

$$6\mathscr{F}_{\mathrm{IMS}}(\phi) = \frac{1}{2}\left(\sum_{\alpha} |\langle \alpha, \phi \rangle|^3 - \sum_i \sum_{\varpi \in \mathbf{R}_i} n_{\mathbf{R}_i} |\langle \varpi, \phi \rangle|^3 \right). \tag{5.1}$$

For all simple groups with the exception of $\mathrm{SU}(N)$ with $N \geq 3$, this is the full purely cubic sector of the prepotential as there are no non-trivial third Casimir invariants.

The *open dual fundamental Weyl chamber* is defined as the cone $\langle \alpha, \phi \rangle > 0$, where α runs through the set of all simple positive roots. This choice makes it possible to remove the absolute values in the sum over the roots. For a given choice of a group G and representations $\mathbf{R}_i$, we then consider the hyperplane arrangement $\langle \varpi, \phi \rangle = 0$, where ϖ runs through all the weights of all the representations $\mathbf{R}_i$ and ϕ is an element of the coroot space. If none of these hyperplanes intersect the interior of the dual Weyl chamber of $\mathfrak{g}$, we can safely remove the absolute values in the sum over the weights.

Otherwise, we have hyperplanes partitioning the dual fundamental Weyl chamber into subchambers. Each of these subchambers is defined by the signs of the linear forms $\langle \varpi, \phi \rangle$ and corresponds to a specific sector of the Coulomb branch. Two such subchambers are adjacent when they differ by the sign of a unique linear form. Within each of these subchambers, the prepotential is a cubic polynomial. But as we go from one subchamber to an adjacent one, we have to go through one of the walls defined by the weights. The transition from one chamber to an adjacent chamber is a phase transition.

5.1 Prepotential and Coulomb phases

It is immediate to compute the prepotential for a gauge theory with gauge group E_7 coupled to n_A hypermultiplets tranforming in the adjoint representation and n_F hypermultiplets transforming in the fundamental representation **56**.

First we recall that the open dual fundamental Weyl chamber is in our conventions given by the seven inequalities $\langle \alpha_i, \phi \rangle$ for $i = 1, \ldots, 7$:

$$\begin{cases} 2\phi_1 - \phi_2 > 0, \quad -\phi_1 + 2\phi_2 - \phi_3 > 0, \quad -\phi_2 + 2\phi_3 - \phi_4 - \phi_7 > 0, \quad -\phi_3 + 2\phi_4 - \phi_5 > 0, \\ -\phi_4 + 2\phi_5 - \phi_6 > 0, \quad 2\phi_6 - \phi_5 > 0, \quad 2\phi_7 - \phi_3 > 0. \end{cases} \tag{5.2}$$

Each of the eight chambers of $\mathrm{I}(\mathrm{E}_7, \mathbf{56})$ is uniquely defined by the signs taken by the seven linear functions $\langle \varpi_i, \phi \rangle$ for $i = \{19, 20, 23, 26, 29, 32, 30\}$. These are classified in Table 1. Imposing these signs together with the condition of being inside the open dual Weyl chamber defines each chamber. We can then compute the prepotential for each chamber: as by their very definition they resolve the absolute values in the definition of $\mathscr{F}(\phi)$, we end up with polynomials. We illustrate the process for Chamber 5. The signs defining Chamber 5 are $(+,+,+,+,-,-,-)$.

$$\begin{cases} \phi_1 - \phi_6 > 0 \quad -\phi_1 + \phi_2 - \phi_6 > 0 \quad -\phi_2 + \phi_3 - \phi_6 > 0 \quad -\phi_3 + \phi_4 - \phi_6 + \phi_7 > 0 \\ -\phi_4 + \phi_5 - \phi_6 + \phi_7 < 0 \quad \phi_7 - \phi_5 < 0 \quad \phi_4 - \phi_6 - \phi_7 < 0 \end{cases} \tag{5.3}$$

We can then immediately compute the prepotential $\mathscr{F}_5(\phi)$:

$$\begin{aligned} 6\mathscr{F}_5(\phi) = {} & 8(1-n_A)(\phi_1^3 + \phi_2^3 + \phi_3^3 + \phi_5^3) + (8(1-n_A) - 2n_F)(\phi_4^3 + \phi_6^3 + \phi_7^3) \\ & + 6(1 - n_A - n_F)(\phi_2\phi_1^2 - \phi_2\phi_3^2) + 6(2n_A + n_F - 2)\phi_2^2\phi_1 \\ & + 6(n_A - n_F - 1)\left(\phi_3^2\phi_4 + \phi_3^2\phi_7 - 2\phi_5\phi_6^2\right) + 6\phi_5^2\phi_6(3n_A - 2n_F - 3) \\ & + 6(1-n_A)\phi_4\left(\phi_5^2 - 2\phi_4\phi_5\right) - 6n_F\phi_4^2(\phi_6 + \phi_7) + 12n_F\phi_4\phi_6\phi_7 \\ & - 6n_F\left(\phi_3\phi_2^2 - \phi_3\phi_4^2 - \phi_3\phi_7^2 + \phi_6\phi_7^2 + \phi_6^2\phi_7 - 2\phi_3\phi_4\phi_7 - 2\phi_4\phi_6\phi_5 + \phi_4\phi_6^2 + \phi_4\phi_7^2\right). \end{aligned} \tag{5.4}$$

5.2 Counting charged hypermultiplets in $5d$ using triple intersection numbers

We can compute the number of charged hypermultiplets by comparing the triple intersection numbers with $6\mathscr{F}_{IMS}(\varphi)$.

We illustrate the process in Chamber 5. We can compute the number of multiplets in the adjoint and the fundamental representations by just computing the intersection numbers D_1^3 and D_4^3 as

the coefficients of ϕ_1^3 and ϕ_4^3 depends on linearly on n_A and n_F and are supposed to match the intersection numbers D_1^3 and D_4^3. Since D_1 is a ruled surface over a curve of genus g and D_4 is the blowup at $S \cdot V(a)$ of a ruled surface over a curve of genus g we have $D_1^3 = 8(1-g)$ and $D_4^3 = 8(1-g) - S \cdot V(a)$. Thus

$$n_A = g, \quad n_F = \frac{1}{2} S \cdot V(a). \tag{5.5}$$

Since the class of a is $[a] = -4K - 3S$, and $KS = 2g - 2 - S^2$, we conclude that

$$n_A = g, \quad n_F = \frac{1}{2}\Big(8(1-g) + S^2\Big). \tag{5.6}$$

We can apply the same technique with the same result in the other chambers as the number of multiplets does not change between different phases of the Coulomb branch.

In the next section, we will see that the same numbers n_A and n_F are required to cancel anomalies of a $\mathcal{N} = (1,0)$ six-dimensional theory obtained from a compactification of F-theory on a Calabi-Yau variety that is a crepant resolution of the Weierstrass model of an E_7-model.

6 Application to $\mathcal{N} = (1,0)$ six-dimensional theories

Local anomalies in six-dimensional theories can be used to constrain the number of charged hypermultiplets. In the best cases, anomaly conditions can even completely fix the matter content of a given six-dimensional theory. This was already brilliantly illustrated by Seiberg just after the first string revolution in a paper in which the absence of anomalies was used to derive the number of matter multiplets in a six-dimensional superconformal field theory [55].

6.1 Anomaly cancellations in $\mathcal{N} = (1,0)$ six-dimensional theories

Here, we consider a $(1,0)$ supersymmetric gauged supergravity theory. Such theories have chiral spinors and chiral tensors and have potential gravitational, gauged, and mixed local anomalies. These local anomalies can be cancelled by the Green-Schwarz mechanism. F-theory compactified on a Calabi-Yau threefold gives a $(1,0)$ supersymmetric six-dimensional gauged supergravity for which the Green-Schwarz mechanism was studied by Sadov [52], see also [36,49,50]. In what follows, R represents the Riemann curvature of spacetime and $\mathrm{tr}\, R^n$ are computed with respect to the fundamental representation of SO(5,1). We denote by n_T, $\mathrm{n}_V^{(6)}$, and n_H the number of tensor, vector, and hypermultiplets, respectively. The gauge group is G and charged hypermultiplets transform in representations $\mathbf{R_i}$ of the gauge group. We can distinguish two types of hypermultiplets: those that are neutral and those that transform under some representation $\mathbf{R_i}$ of the gauge group. In our conventions, hypermultiplets that are charged under a zero weight of the representation are considered neutral.

The relevant trace identities for E_7 are [19]

$$\mathrm{tr}_{\mathbf{133}}\, F^2 = 3\,\mathrm{tr}_{\mathbf{56}}\, F^2, \quad \mathrm{tr}_{\mathbf{133}}\, F^4 = \frac{1}{6}(\mathrm{tr}_{\mathbf{56}}\, F^2)^2, \quad \mathrm{tr}_{\mathbf{56}}\, F^4 = \frac{1}{24}(\mathrm{tr}_{\mathbf{56}}\, F^2)^2, \tag{6.1}$$

where we note that E_7 does not have an independent fourth Casimir invariant. The trace identities

for a representation $\mathbf{R}_i$ of a simple group G are

$$\mathrm{tr}_{\mathbf{R_i}}\, F_a^2 = A_{\mathbf{R_i}}\, \mathrm{tr}_{\mathbf{F}}\, F^2, \quad \mathrm{tr}_{\mathbf{R_i}}\, F^4 = B_{\mathbf{R_i}}\, \mathrm{tr}_{\mathbf{F}}\, F^4 + C_{\mathbf{R_i}} (\mathrm{tr}_{\mathbf{F}}\, F^2)^2, \tag{6.2}$$

with respect to a reference representation $\mathbf{F}$ that we can freely choose. We take it to be the fundamental representation. These group theoretical coefficients are listed in [19].

The anomalies are canceled by the Green-Schwarz mechanism when I_8 factorizes [37,53,54]. The modification of the field strength H of the antisymmetric tensor B is

$$H = dB + \frac{1}{2} K \omega_{3L} + \frac{2}{\lambda} S \omega_{a,3Y}, \tag{6.3}$$

where ω_{3L} and $\omega_{a,3Y}$ are respectively the gravitational and Yang-Mills Chern-Simons terms. If I_8 factors as

$$\mathrm{I}_8 = X \cdot X, \tag{6.4}$$

then the anomaly is canceled by adding the following Green-Schwarz counter-term

$$\Delta L_{GS} \propto \frac{1}{2} B \wedge X. \tag{6.5}$$

Following Sadov [52], to cancel the local anomalies, we consider

$$X = \frac{1}{2} K\, \mathrm{tr}\, R^2 + \frac{2}{\lambda} S\, \mathrm{tr}\, F^2, \tag{6.6}$$

where λ is a constant normalization factor chosen such that the smallest topological charge of an embedded SU(2) instanton in the gauge group G is one [8, 44, 50]. This forces λ to be the Dynkin index of the fundamental representation of G as listed in Table 4 [50].

If the simple group G is supported on a divisor S, the local anomaly cancellation conditions are the following equations [8, 44, 50, 52]

$$n_T = 9 - K^2, \tag{6.7a}$$

$$n_H - n_V^{(6)} + 29 n_T - 273 = 0, \tag{6.7b}$$

$$\left(B_{\mathbf{adj}} - \sum_i n_{\mathbf{R_i}} B_{\mathbf{R_i}} \right) = 0, \tag{6.7c}$$

$$\lambda \left(A_{\mathbf{adj}} - \sum_i n_{\mathbf{R_i}} A_{\mathbf{R_i}} \right) = 6 K \cdot S, \tag{6.7d}$$

$$\lambda^2 \left(C_{\mathbf{adj}} - \sum_i n_{\mathbf{R_i}} C_{\mathbf{R_i}} \right) = -3 S^2. \tag{6.7e}$$

The first equation gives us the number of tensor multiplets n_T. The second equation is the vanishing of the coefficient of $\mathrm{tr}\, R^4$ and will be checked at the end. The third equation is automatically satisfied since E_7 has no independent quartic Casimir (and therefore all the coefficients B_{adj} and B_i are zero).

The total number of hypermultiplets is the sum of the neutral hypermultiplets and the charged

$\mathfrak{g}$	A_n	B_n	C_n	D_n	E_8	E_7	E_6	F_4	G_2
λ	1	2	1	2	60	12	6	6	2

Table 4: The normalization factors for each simple gauge algebra. See [44].

hypermultiplets. For a compactification on a Calabi-Yau threefold Y, the number of neutral hypermultiplets is $n_H^0 = h^{2,1}(Y) + 1$ [13]. The number of each multiplet is [13, 36]

$$n_V^{(6)} = \dim G, \quad n_T = h^{1,1}(B) - 1 = 9 - K^2, \tag{6.8}$$

$$n_H = n_H^0 + n_H^{ch} = h^{2,1}(Y) + 1 + \sum_i n_{\mathbf{R_i}} \left(\dim \mathbf{R_i} - \dim \mathbf{R_i^{(0)}} \right), \tag{6.9}$$

where the (elliptically-fibered) base B is a rational surface with canonical class K. Here, $\mathrm{n}_{\mathbf{R_i}}$ is the number of hypermultiplets transforming non-trivially in the representation $\mathbf{R_i}$ of the gauge group, $\dim \mathbf{R_i^{(0)}}$ is the number of zero weights in the representation $\mathbf{R_i}$.

6.2 Counting hypermultiplets in $6d$ using anomaly cancellation conditions

With the gauge group E_7, we have $n_V^{(6)} = 133$ and $h^{2,1}(Y)$ was computed in [26] for any crepant resolution of a Weierstrass model of an E_7-model:

$$n_V^{(6)} = 133, \quad h^{2,1}(Y) = 18 + 29K^2 + 49K \cdot S + 21S^2. \tag{6.10}$$

For E_7, the normalization factor λ is 12. Since we have a unique component in the gauge group, the anomaly equations are:

$$12(3 - 3n_{\mathbf{133}} - n_{\mathbf{56}}) = 6K \cdot S, \quad 12^2(\frac{1}{6} - \frac{1}{6}n_{\mathbf{133}} - \frac{1}{24}n_{\mathbf{56}}) = -3S^2. \tag{6.11}$$

Using the identity $2 - 2g = -K \cdot S - S^2$, where g is the arithmetic genus of the curve S, we find:

$$n_{\mathbf{133}} = g, \quad n_{\mathbf{56}} = \frac{1}{2}(8 - 8g + S^2), \tag{6.12}$$

which matches what we found by comparing the triple intersection numbers with the prepotential in the $\mathcal{N} = 1$ five-dimensional theory obtained by compactifiying M-theory on the same elliptic fibration.

The total number of hypermultiplets is then

$$n_H = (18 + 29K^2 + 49K \cdot S + 21S^2) + 1 + (133 - 7)n_{\mathbf{133}} + 56n_{\mathbf{56}} = 29(5 + K^2). \tag{6.13}$$

Using equations (6.12) and (6.13), it is a simple arithmetic computation to check that the coefficient of $\mathrm{tr}\, R^4$ vanishes identically [51]:

$$n_H - n_V^{(6)} + 29n_T - 273 = 0. \tag{6.14}$$

Remark 6.1. As explained in the introduction, the value of $n_{\mathbf{56}}$ computed in (6.12) equals one-half of the intersection number $S \cdot V(a)$, which is the number of points over which the fiber III^* degenerates to an incomplete fiber of type II^*. The number is a half-integer when S has odd self-intersection. If S is a rational curve, we see that requesting $n_{\mathbf{56}}$ to be non-negative forces the self-intersection number S^2 to be greater or equal to -8. A rational curve with self-intersection $-n$ $(n > 0)$ is called a $-n$-curve. When S is a -8-curve, S does not intersect $V(a)$ and there is no matter in the representation **56**. When S is a -7-curve, S intersects $V(a)$ at exactly one point and we get one half-hypermultiplet in the representation **56**.

Acknowledgements

M.E. is supported in part by the National Science Foundation (NSF) grant DMS-1701635 "Elliptic Fibrations and String Theory." S.P. is supported by the National Science Foundation through a Graduate Research Fellowship under grant DGE-1144152 and by the Hertz Foundation through a Harold and Ruth Newman Fellowship.

A Relevant Definitions

Definition A.1. An *elliptic fibration* is a projective surjective morphism $\varphi : X \longrightarrow B$ between normal varieties such that φ is proper and endowed with a rational section[5] and the fiber over the generic point of B is a regular projective curve of genus one.

Definition A.2. The *discriminant locus* of an elliptic fibration $\varphi : X \longrightarrow B$ is the locus of points p such that the fiber over p is a singular fiber. Under mild assumptions, the discriminant locus is a divisor in the base. The prime components of the pre-image of prime components of the discriminant locus are called *fibral divisors*.

Definition A.3 ($\mathbb{Q}$-Gorenstein, $\mathbb{Q}$-factorial, nef-divisors)**.**

1. A prime Weil divisor D is said to be $\mathbb{Q}$-Cartier when some integral multiple of D is a Cartier divisor.
2. A variety Y is said to be $\mathbb{Q}$-*Gorenstein* if its canonical class is $\mathbb{Q}$-Cartier.
3. A normal variety Y is said to be $\mathbb{Q}$-*factorial* if every prime Weil divisor D on X is $\mathbb{Q}$-Cartier.
4. Let $f : Y \longrightarrow X$ be a projective morphism between normal varieties. A divisor D is said to be *f-nef (or relatively nef over S)* when $\int_Y D \cdot C \geq 0$ for any curve C projected to a point by f.

Definition A.4 (Minimal models)**.** A *minimal model* of a projective morphism $f : Y \longrightarrow S$ between quasi-projective normal varieties is a projective morphism $f' : Y' \longrightarrow S$ such that

1. There exists a birational map $\alpha : Y' \dashrightarrow Y$ such that $f' = f \circ \alpha$.

[5] Given a surjective morphism $\varphi : X \to B$, a rational section is a rational map $\sigma : B \longrightarrow X$ such that $\varphi \circ \sigma$ is the identity away from a Zariski closed set of X.

2. Y' has only $\mathbb{Q}$-factorial terminal singularities.

3. $K_{Y'}$ is f'-nef.

Definition A.5 (Modifications, (crepant) resolutions of singularities)**.**

1. A *modification* of a variety X is a proper birational morphism $f : \widetilde{X} \longrightarrow X$.

2. A *resolution* of a singularity is a modification $f : \widetilde{X} \longrightarrow X$ such that $\widetilde{X}$ is nonsingular.

3. A resolution $f : \widetilde{X} \longrightarrow X$ is said to be *crepant* when X is $\mathbb{Q}$-Gorenstein and f preserves the canonical class of X ($K_{\widetilde{X}} = \varphi^* K_X$).

4. A *strong resolution* is a resolution that is an isomorphism away from the singular locus, that is, a resolution $f : \widetilde{X} \longrightarrow X$ such that the restriction of f to $\widetilde{X} \backslash f^{-1}(Sing(X))$ is an isomorphism onto $X \backslash Sing(X)$.

In this paper we only consider strong resolutions and simply call them *resolutions*.

Remark A.6. A crepant resolution of Y is automatically a nonsingular minimal model over Y. Distinct crepant resolutions are connected by a chain of flops if we assume the existence and the termination of flops. Kawamata has shown [41] that the seminal results of Birkar-Cascini-Hacon-McKernan [12] together with the boundedness of length of extremal rays imply that different minimal models are connected by a sequence of flops.

A variety can be $\mathbb{Q}$-factorial in the projective category but fail to be $\mathbb{Q}$-factorial in the analytic category. An important consequence of the following lemma is that terminal $\mathbb{Q}$-factorial singularities are obstructions to the existence of a crepant resolution.

Lemma A.7 (See [43, Corollary 2.63])**.** *Let $f : Y \to X$ be a birational morphism between normal varieties. If X is $\mathbb{Q}$-factorial, then the exceptional locus of f is of pure codimension one.*

References

[1] P. Aluffi and M. Esole. Chern class identities from tadpole matching in type IIB and F-theory. *JHEP*, 03:032, 2009.

[2] P. Aluffi and M. Esole. New Orientifold Weak Coupling Limits in F-theory. *JHEP*, 02:020, 2010.

[3] L. B. Anderson, M. Esole, L. Fredrickson and L. P. Schaposnik, "Singular Geometry and Higgs Bundles in String Theory," SIGMA **14**, 037 (2018) [arXiv:1710.08453 [math.DG]].

[4] P. S. Aspinwall and M. Gross, "The SO(32) heterotic string on a K3 surface," Phys. Lett. B **387**, 735 (1996) doi:10.1016/0370-2693(96)01095-7 [hep-th/9605131].

[5] P. S. Aspinwall, S. H. Katz and D. R. Morrison, "Lie groups, Calabi-Yau threefolds, and F theory," Adv. Theor. Math. Phys. **4**, 95 (2000) [hep-th/0002012].

[6] L. Bhardwaj and P. Jefferson, "Classifying 5d SCFTs via 6d SCFTs: Rank one," arXiv:1809.01650 [hep-th].

[7] V. V. Batyrev. Birational Calabi-Yau n-folds have equal Betti numbers. In *New trends in algebraic geometry (Warwick, 1996)*, volume 264 of *London Math. Soc. Lecture Note Ser.*, pages 1–11. Cambridge Univ. Press, Cambridge, 1999.

[8] C. W. Bernard, N. H. Christ, A. H. Guth and E. J. Weinberg, Instanton Parameters for Arbitrary Gauge Groups, Phys. Rev. D **16**, 2967 (1977).

[9] M. Bershadsky, K. A. Intriligator, S. Kachru, D. R. Morrison, V. Sadov, and C. Vafa. Geometric singularities and enhanced gauge symmetries. *Nucl. Phys.*, B481:215–252, 1996.

[10] R. Borcherds. Lie Groups. https://math.berkeley.edu/∼reb/courses/261/all.pdf (updated May 25, 2012).

[11] N. Bourbaki, *Groups and Lie Algebras. Chap. 4–6*, Translated from the 1968 French original. Elements of Mathematics (Berlin). Springer-Verlag, Berlin Heidelberg, 2002.

[12] C. Birkar, P. Cascini, C. D. Hacon, and J. McKernan, *Existence of minimal models for varieties of log general type*, math.AG/0610203.

[13] A. C. Cadavid, A. Ceresole, R. D'Auria and S. Ferrara, "Eleven-dimensional supergravity compactified on Calabi-Yau threefolds," Phys. Lett. B **357**, 76 (1995) doi:10.1016/0370-2693(95)00891-N [hep-th/9506144].

[14] P. Candelas, D. E. Diaconescu, B. Florea, D. R. Morrison and G. Rajesh, Codimension three bundle singularities in F theory, JHEP **0206**, 014 (2002) doi:10.1088/1126-6708/2002/06/014.

[15] A. Collinucci, F. Denef, and M. Esole. D-brane Deconstructions in IIB Orientifolds. *JHEP*, 02:005, 2009.

[16] P. Deligne. Courbes elliptiques: formulaire d'après J. Tate. In *Modular functions of one variable, IV (Proc. Internat. Summer School, Univ. Antwerp, Antwerp, 1972)*, pages 53–73. Lecture Notes in Math., Vol. 476. Springer, Berlin, 1975.

[17] M. Del Zotto, J. J. Heckman and D. R. Morrison, "6D SCFTs and Phases of 5D Theories," arXiv:1703.02981 [hep-th].

[18] D. E. Diaconescu and R. Entin, "Calabi-Yau spaces and five-dimensional field theories with exceptional gauge symmetry," Nucl. Phys. B **538**, 451 (1999) doi:10.1016/S0550-3213(98)00689-0 [hep-th/9807170].

[19] J. Erler, Anomaly cancellation in six-dimensions, J. Math. Phys. **35**, 1819 (1994)

[20] M. Esole, "Introduction to Elliptic Fibrations," doi:10.1007/978-3-319-65427-07

[21] M. Esole, J. Fullwood, and S.-T. Yau. D_5 elliptic fibrations: non-Kodaira fibers and new orientifold limits of F-theory. Commun. Num. Theor. Phys. **09**, no. 3, 583 (2015) doi:10.4310/CNTP.2015.v9.n3.a4 [arXiv:1110.6177 [hep-th]].

[22] M. Esole, S. G. Jackson, R. Jagadeesan, and A. G. Noël. Incidence Geometry in a Weyl Chamber I: GL_n, arXiv:1508.03038 [math.RT].

[23] M. Esole, S. G. Jackson, R. Jagadeesan, and A. G. Noël. Incidence Geometry in a Weyl Chamber II: SL_n. 2015. arXiv:1601.05070 [math.RT].

[24] M. Esole, R. Jagadeesan and M. J. Kang, The Geometry of G_2, Spin(7), and Spin(8)-models, arXiv:1709.04913 [hep-th].

[25] M. Esole, P. Jefferson and M. J. Kang, "The Geometry of F_4-Models," arXiv:1704.08251 [hep-th].

[26] M. Esole, P. Jefferson and M. J. Kang, "Euler Characteristics of Crepant Resolutions of Weierstrass Models," arXiv:1703.00905 [math.AG].

[27] M. Esole and M. J. Kang, Characteristic numbers of crepant resolutions of Weierstrass models, arXiv:1807.08755 [hep-th].

[28] M. Esole and M. J. Kang, "The Geometry of the $\mathrm{SU}(2)\times \mathrm{G}_2$-model," arXiv:1805.03214 [hep-th].

[29] M. Esole and M. J. Kang, "Flopping and Slicing: SO(4) and Spin(4)-models," arXiv:1802.04802 [hep-th].

[30] M. Esole, M. J. Kang and S. T. Yau, "Mordell-Weil Torsion, Anomalies, and Phase Transitions," arXiv:1712.02337 [hep-th].

[31] M. Esole, M. J. Kang, and S.-T. Yau. A New Model for Elliptic Fibrations with a Rank One Mordell-Weil Group: I. Singular Fibers and Semi-Stable Degenerations. 2014.

[32] M. Esole and R. Savelli, Tate Form and Weak Coupling Limits in F-theory,' JHEP **1306**, 027 (2013).

[33] M. Esole, S.-H. Shao, and S.-T. Yau. Singularities and Gauge Theory Phases. *Adv. Theor. Math. Phys.*, 19:1183–1247, 2015.

[34] M. Esole, S.-H. Shao, and S.-T. Yau. Singularities and Gauge Theory Phases II. *Adv. Theor. Math. Phys.*, 20:683–749, 2016.

[35] M. Esole and S.-T. Yau. Small resolutions of SU(5)-models in F-theory. *Adv. Theor. Math. Phys.*, 17:1195–1253, 2013.

[36] A. Grassi and D. R. Morrison. Group representations and the Euler characteristic of elliptically fibered Calabi-Yau threefolds. *J. Algebraic Geom.*, 12(2):321–356, 2003.

[37] M. B. Green, J. H. Schwarz and P. C. West, "Anomaly Free Chiral Theories in Six-Dimensions," Nucl. Phys. B **254**, 327 (1985).

[38] H. Hayashi, C. Lawrie, D. R. Morrison, and S. Schafer-Nameki. Box Graphs and Singular Fibers. *JHEP*, 1405:048, 2014.

[39] K. A. Intriligator, D. R. Morrison, and N. Seiberg. Five-dimensional supersymmetric gauge theories and degenerations of Calabi-Yau spaces. *Nucl.Phys.*, B497:56–100, 1997.

[40] S. Katz, D. R. Morrison, S. Schafer-Nameki, and J. Sully. Tate's algorithm and F-theory. *JHEP*, 1108:094, 2011.

[41] Y. Kawamata. Flops Connect Minimal Models. *Publ. Res. Inst. Math. Sci.* 44 (2008), 419-423.

[42] K. Kodaira. On compact analytic surfaces. II, III. *Ann. of Math. (2) 77 (1963), 563–626; ibid.*, 78:1–40, 1963.

[43] J. Kollár and S. Mori, *Birational Geometry of Algebraic Varieties*, Cambridge Univ. Press, Cambridge, 1998.

[44] V. Kumar, D. R. Morrison and W. Taylor, Global aspects of the space of 6D N = 1 supergravities, JHEP **1011**, 118 (2010)

[45] K. Matsuki, Introduction to the Mori Program. Springer Science & Business Media, 2013.

[46] D. R. Morrison and M. R. Plesser, "Nonspherical horizons. 1.," Adv. Theor. Math. Phys. **3**, 1 (1999)

[47] D. R. Morrison and W. Taylor, Classifying bases for 6D F-theory models, Central Eur. J. Phys. **10**, 1072 (2012).

[48] A. Néron. Modèles minimaux des variétés abéliennes sur les corps locaux et globaux. *Inst. Hautes Études Sci. Publ.Math. No.*, 21:128, 1964.

[49] S. Monnier, G. W. Moore and D. S. Park, Quantization of anomaly coefficients in 6D $\mathcal{N} = (1, 0)$ supergravity, JHEP **1802**, 020 (2018)

[50] D. S. Park, Anomaly Equations and Intersection Theory, JHEP **1201**, 093 (2012)

[51] S. Randjbar-Daemi, A. Salam, E. Sezgin and J. A. Strathdee, An Anomaly Free Model in Six-Dimensions, Phys. Lett. **151B**, 351 (1985)

[52] V. Sadov, Generalized Green–Schwarz mechanism in F theory, Phys. Lett. B **388**, 45 (1996).

[53] A. Sagnotti, A Note on the Green-Schwarz mechanism in open string theories, Phys. Lett. B **294**, 196 (1992).

[54] J. H. Schwarz, Anomaly-free supersymmetric models in six dimensions, Phys. Lett. B **371**, 223 (1996).

[55] N. Seiberg, "Observations on the Moduli Space of Superconformal Field Theories," Nucl. Phys. B **303**, 286 (1988).

[56] J. Tate. Algorithm for determining the type of a singular fiber in an elliptic pencil. In *Modular functions of one variable, IV (Proc. Internat. Summer School, Univ. Antwerp, Antwerp, 1972)*, pages 33–52. Lecture Notes in Math., Vol. 476. Springer, Berlin, 1975.